Debris Mobility of Failures within Topographic Depression Catchments

GEO Report No. 361

F.L.C. Lo, J.S.H. Kwan, F.W.Y. Ko & H.Y. Ho

Geotechnical Engineering Office
Civil Engineering and Development Department
The Government of the Hong Kong
Special Administrative Region

Debris Mobility of Failures within Topographic Depression Catchments

GEO Report No. 361

F.L.C. Lo, J.S.H. Kwan, F.W.Y. Ko & H.Y. Ho

This report was originally produced in October 2013
as GEO Special Project Report No. SPR 2/2013

First published, December 2022

Prepared by:

Geotechnical Engineering Office,
Civil Engineering and Development Department,
Civil Engineering and Development Building,
101 Princess Margaret Road,
Homantin, Kowloon,
Hong Kong.

Preface

In keeping with our policy of releasing information which may be of general interest to the geotechnical profession and the public, we make available selected internal reports in a series of publications termed the GEO Report series. The GEO Reports can be downloaded from the website of the Civil Engineering and Development Department (http://www.cedd.gov.hk) on the Internet.

Raymond WM Cheung
Head, Geotechnical Engineering Office
December 2022

Foreword

This Report documents the methodology and results of a study of debris mobility of failures within topographic depression catchments (TDF), and the recommendations pertinent to the methods and rheological model to be used for the debris mobility assessments of TDF.

This study was undertaken by Mr Frankie Lo, Ms Florence Ko and Dr Julian Kwan. As part of the study, a series of aerial photograph interpretations was carried out by Ms Hoi-yan Ho, Ms Hei-yin Wong and Mr Willie Shum. Technical Officer, Mr Wai-kit Ho, provided technical support in conducting the back analyses. Drafting unit of the Standards and Testing Division assisted in formatting this report.

Y.K. Shiu
Chief Geotechnical Engineer/Standards & Testing

Abstract

A study has been carried out to examine the debris mobility of failures in topographic depression catchments (TDF). In the study, 46 historical mobile TDF were identified and back analysed using computer program 2d-DMM. The methodology adopted in identifying the TDF, the assumptions made in the back analyses and results of the study are documented in this Report. Recommendations pertinent to debris mobility assessments of TDF are also included.

This study revealed that mobility analyses using Voellmy parameters ϕ_a = 18° and ξ = 1000 m/s^2 produce suitably conservative estimates of runout distances of most of the mobile TDF, and that debris velocities match reasonably well with those of a historical TDF in Kau Lung Hang Shan. It is recommended that the rheological parameters should be adopted for forward prediction purposes. However, where historical landslides in the TD catchments of concerned have resulted in more mobile debris runout than that assessed using the above recommended rheological parameters, the appropriate rheological parameters to be adopted in analytical design of TDF mitigation measures should be assessed on a case-by-case basis.

Contents

		Page No.
Title Page		1
Preface		3
Foreword		4
Abstract		5
Contents		6
List of Table		7
List of Figures		8
1	Introduction	9
2	Methodology of the Study	9
3	Mobility Analyses of TDF	12
	3.1 Results of Analyses	12
	3.2 Benchmarking against the Kau Lung Hang Shan TDF	14
	3.3 Effect of Source Volume	16
4	Discussion	17
5	Conclusions and Recommendations	17
6	References	18
Appendix A:	Classification of Hillside Catchments Extracted from GEO TGN 36	20
Appendix B:	List of Mobile Failures within Topographic Depression Catchments Identified in ENTLI	25
Appendix C:	Topographic Plans of Mobile Failures within Topographic Depression Catchments Identified in ENTLI	29

List of Table

Table No.		Page No.
2.1	Rheological Parameters Used in Mobility Analyses of the 46 TDF	11

List of Figures

Figure No.		Page No.
2.1	Summary of the Number of Cases Involved in the Identification Process	10
2.2	The tanϕ_a -1/ξ Space	11
3.1	Comparison of Calculated Runout Distance and Actual Runout Distance based on API	13
3.2	Estimation of Runout Distance Using ϕ_a = 18°, ξ = 1000 m/s^2	13
3.3	Under-estimation of Runout Distances Using ϕ_a = 18°, ξ = 1000 m/s^2	14
3.4	The Kau Lung Hang Shan Failure (GEO, 2006)	14
3.5	Calculated Debris Velocity Profile and Estimated Debris Velocities	15
3.6	Cumulative Percentage of the 46 TDF in Terms of Source Volume	16
3.7	Runout Distances Estimated Using ϕ_a = 18°, ξ = 1000 m/s^2 According to Landslide Volumes	17

1 Introduction

Ng et al (2003) described two main types of natural terrain landslide hazards in Hong Kong, viz. channelized debris flows (CDF) and open hillslope landslides (OHL). CDF occur in well-defined, incised natural drainage lines and OHL occur on relatively planar hillsides. Rheological parameters for assessing the mobility of CDF and OHL in Hong Kong are reported by Lo (2000). Updated guidance is given in GEO (2011 & 2012a).

Experience shows that there are cases where the mode of landslide debris transport is somewhat between OHL and CDF as highlighted by Ng et al (2003). Wong et al (2006) introduced an additional hazard type, viz. failures within topographic depressions (TDF), to deal with the intermediate situations between CDF and OHL. Classification of catchments associated with CDF, TDF and OHL is further elaborated in GEO (2013) (see also Appendix A).

Mobility of TDF in Hong Kong was not investigated systematically before, and therefore a study on this subject has been initiated. This report documents the methodology and results of this study. Recommendations pertaining to the mobility assessments of TDF are also given.

2 Methodology of the Study

TDF were first identified from the historical landslides contained in the Enhanced Natural Terrain Landslide Inventory (ENTLI) with data updated to 2009. The more mobile landslides were screened in initially. They included 120 out of about 12,500 recent OHL with runout distance exceeding 100 m and 500 out of about 6,700 recent CDF with runout distance exceeding 175 m. The site settings of these cases were reviewed in detail using LIC 1:1000-scale topographic maps and aerial photographs to establish whether they were genuine TDF in accordance with the technical recommendations given in GEO (2013). Topographic depression catchments cover a broad spectrum, and it is recognized that both LIC topographic maps and aerial photographs have their limitations. Therefore, care has been exercised in identifying TDF. For example, low-flight aerial photographs were used, as far as practicable, and the results of aerial photograph interpretation were reviewed by experienced geologists.

A total of 46 genuine mobile TDF were identified from the above exercise for mobility analysis. Figure 2.1 shows a breakdown of the number of cases involved in the process of identifying the mobile TDF cases. Appendix B lists the corresponding ENTLI number, landslide source dimensions and runout distances of the 46 TDF. The list also includes the aerial photographs reviewed in this study. Appendix C presents the topographic plans of these TDF.

Mobility analysis to simulate the runout dynamics of the TDF was carried out using the computer program 2d-DMM (GEO, 2012b). The runout profiles of the 46 TDF were generated using the 2010 airborne LiDAR survey data for input to 2d-DMM. The landslide source volume was estimated based on the source dimensions recorded in the ENTLI, using the upper-bound empirical correlation suggested by Tattersall et al (2009). Entrainment is assumed to be negligible in the analysis, and the cross-section of debris trail is assumed to be rectangular. The width of debris trail is taken as the source failure width recorded in the

ENTLI unless the width as identified in the aerial photograph is significantly different from that of the ENTLI. Other parameters adopted in the analysis are listed below:

- active pressure coefficient, k_a = 0.8;
- passive pressure coefficient, k_p = 2.5;
- 'at-rest' pressure coefficient, k_o = 1.0; and
- pore-water pressure coefficient, r_u = 0.5.

Savage & Hutter equation as recommended by Pudasaini & Hutter (2007) was used to establish the values of k_a and k_p. According to the equation, the active pressure coefficient and passive pressure coefficient are governed by the values of apparent friction angle (ϕ_a) and bulk friction angle (ϕ_b) of landslide debris. In the present study, ϕ_a ranging from 10° to 30° and ϕ_b ranging from 20° to 35° were adopted. The adopted values of k_a = 0.8 and k_p = 2.5 correspond to the average values of k_a and k_p calculated by the Savage & Hutter equation.

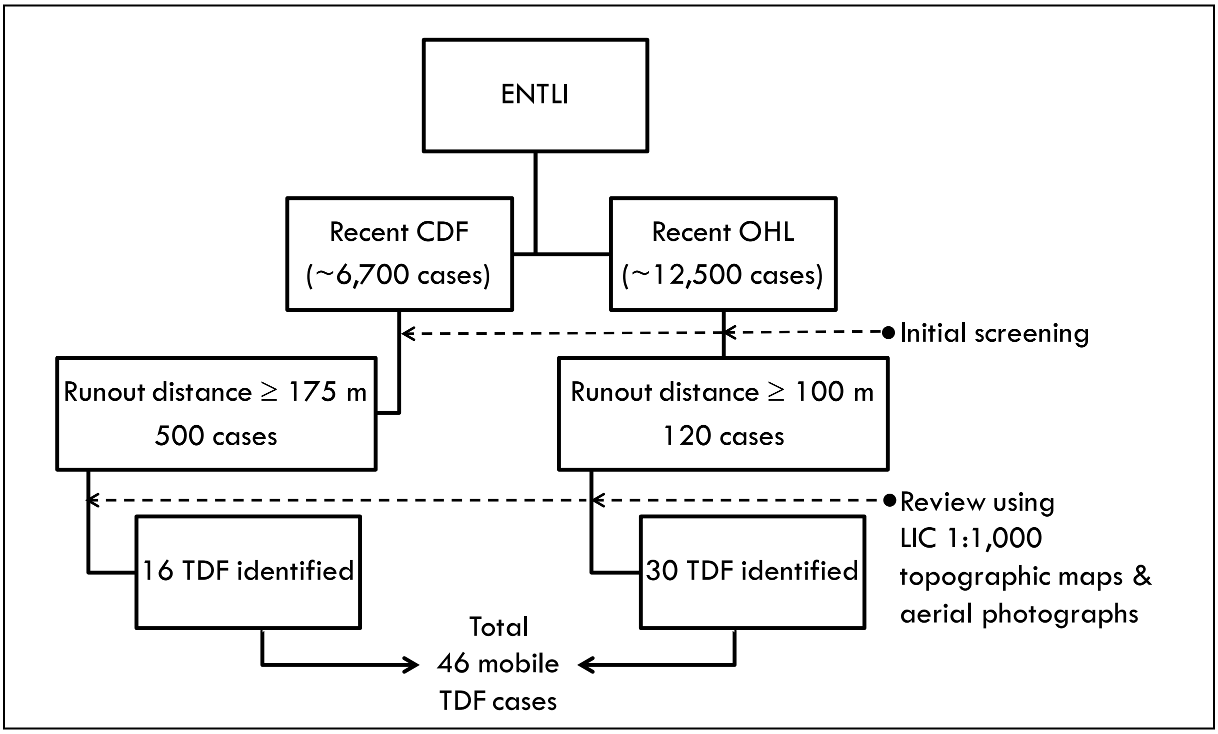

Figure 2.1 Summary of the Number of Cases Involved in the Identification Process

The aim of the present study is not to identify the actual rheological parameters which best describe the mobility of the individual TDF but rather to establish a set of suitably robust rheological parameters for use in forward mobility assessment of TDF (e.g. for the design of natural terrain hazard mitigation measures). According to GEO (2012a), the frictional rheological model should be used for the mobility analysis of OHL and that ϕ_a should be taken as 20° if the landslide volume is larger than or equal to 400 m^3, and ϕ_a = 25° for other landslide volumes. GEO (2011) provides updated guidance on the mobility assessment of CDF. It recommends that the Voellmy model should be used for the mobility assessment of CDF and that ϕ_a and turbulence coefficient ξ should be generally taken as 11° and 500 m/s^2

respectively. Voellmy resistance is proportional to the values of tanϕ_a and $1/\xi$ (i.e. inverse of ξ). Figure 2.2 shows the above recommended rheological parameters for OHL and CDF mobility assessments in the tanϕ_a -$1/\xi$ space.

The mobility analyses for the 46 TDF were carried out based on 10 sets of Voellmy parameters. Each set of the parameters consists of a combination of ϕ_a and ξ as shown in Table 2.1. Those 10 combinations provide a reasonable coverage of the region in the tanϕ_a -$1/\xi$ space bounded by the rheological parameters recommended for mobility assessments of CDF and OHL (see Figure 2.2).

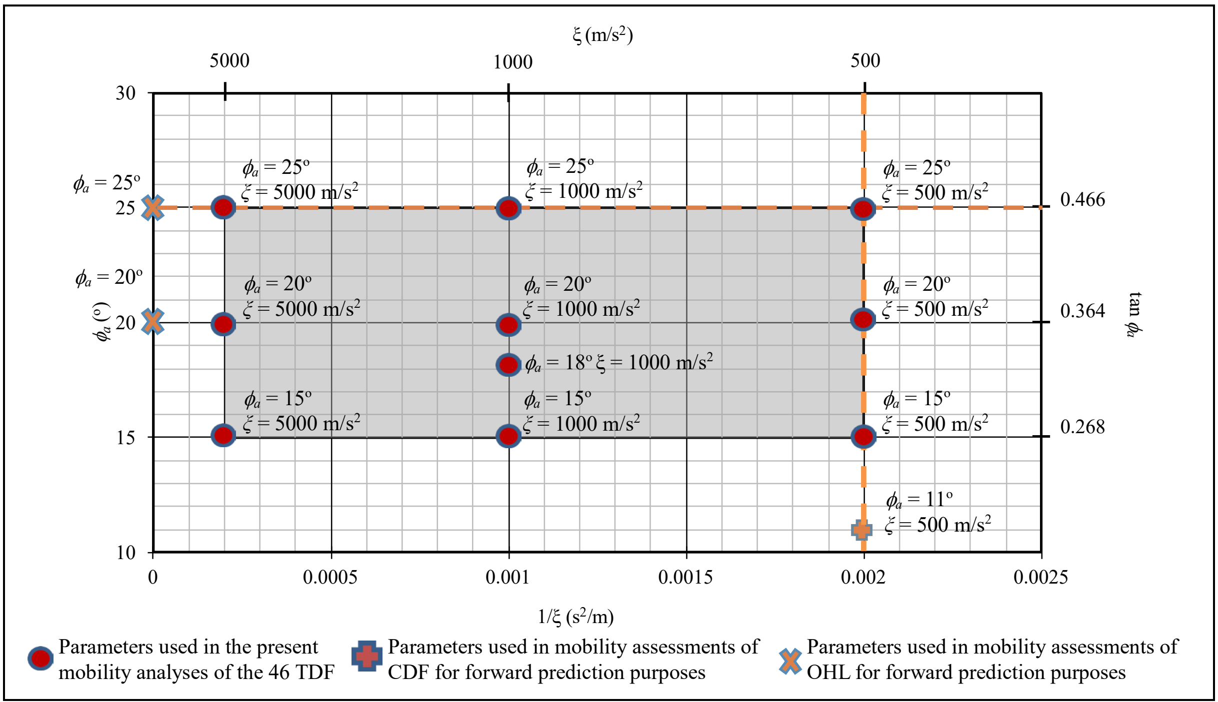

Figure 2.2 The tanϕ_a -$1/\xi$ Space

Table 2.1 Rheological Parameters Used in Mobility Analyses of the 46 TDF

Combination	ϕ_a (tanϕ_a)	ξ
1	15° (0.27)	5000
2	15° (0.27)	1000
3	15° (0.27)	500
4	20° (0.36)	5000
5	18° (0.32)	1000
6	20° (0.36)	1000
7	20° (0.36)	500
8	25° (0.47)	5000
9	25° (0.47)	1000
10	25° (0.47)	500

3 Mobility Analyses of TDF

3.1 Results of Analyses

The calculated debris runout distances of the 46 TDF using the 10 sets of rheological parameters are compared with the debris runout distances as derived from the aerial photographs in this study. The results are presented in Figure 3.1.

Among the 10 sets of rheological parameters considered, the combination of ϕ_a = 25° and ξ = 500 m/s^2 represents the least mobile while the combination of ϕ_a = 15° and ξ = 5000 m/s^2 is the most mobile. The calculated debris runout distances are sensitive to the value of ϕ_a adopted. With the use of the sets of rheological parameters involving ϕ_a = 15°, 2d-DMM over-estimates the runout distance in most of the cases (see lines with squares in Figure 3.1). In contrast, when the sets of rheological parameters involving ϕ_a = 25° are used, the mobility analyses under-estimate the runout distance for many of the cases (see lines with circles). Mobility analyses using 20º-500 m/s^2 and 20º-1000 m/s^2 also produce significant under-estimation in runout distances. The under-estimation could be up to 30% - 40%.

The remaining sets of rheological parameters are 18°-1000 m/s^2 or 20°-5000 m/s^2. The latter parameter set gives relatively a smaller number of cases of under-estimation (four cases). However, the maximum velocity calculated by the mobility analyses using the parameter set 20°-5000 m/s^2 exceeds 15 m/s in 20 out of the 46 cases. Nine of those cases which predicted a high velocity have a landslide source volume of less than 200 m^3. The velocity calculated using the parameter set of 20°-5000 m/s^2 appears to be not consistent with local experience (e.g. the velocity of the 2008 Yu Tung Road Debris Flow estimated based on video recording and mobility analyses is in the range of 10-15 m/s only; the source volume of the Debris Flow exceeded 2400 m^3).

The rheological parameter set of 18°-1000 m/s^2 over-estimates the runout distances of 37 cases, and under-estimates those of the remaining nine cases (Figure 3.2). Out of these nine cases, the runout distance in four cases is under-estimated by less than 5% only (see Figure 3.3). The maximum under-estimation is bounded by 12%. Given the present knowledge, it is not possible to identify the adverse site settings that would give rise to the occurrence of more mobile TDF. However, it should be emphasised that the TDF samples considered in this study belong to a biased dataset because they represent the more mobile historical TDF in the ENTLI. If the dataset of a larger sample size is considered, additional less mobile TDF would be included in the mobility analyses and the percentage of cases with under-estimation of the runout distance would be reduced. Amongst the range of rheological parameters studied, the parameter set with ϕ_a = 18° and ξ = 1000 m/s^2 is considered suitable and sufficiently robust for forward prediction of the mobility of TDF for the design of natural terrain hazard mitigation measures.

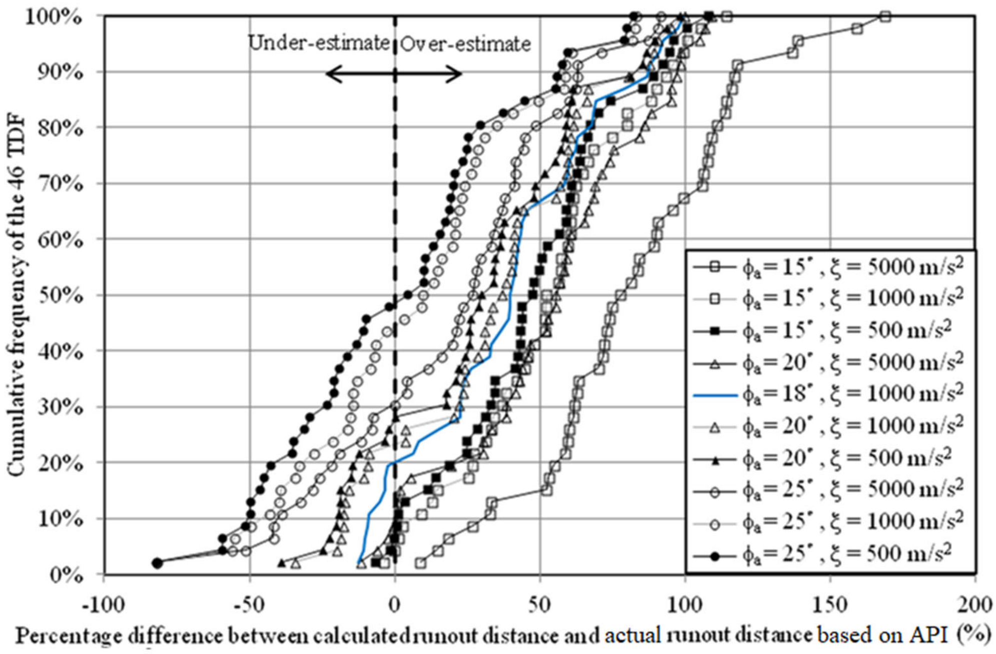

Note: $$\% \text{ difference in runout distance} = \frac{\text{(Calculated runout distance - Actual runout distance based on API)}}{\text{Actual runout distance based on API}} \times 100\%.$$

Figure 3.1 Comparison of Calculated Runout Distance and Actual Runout Distance based on API

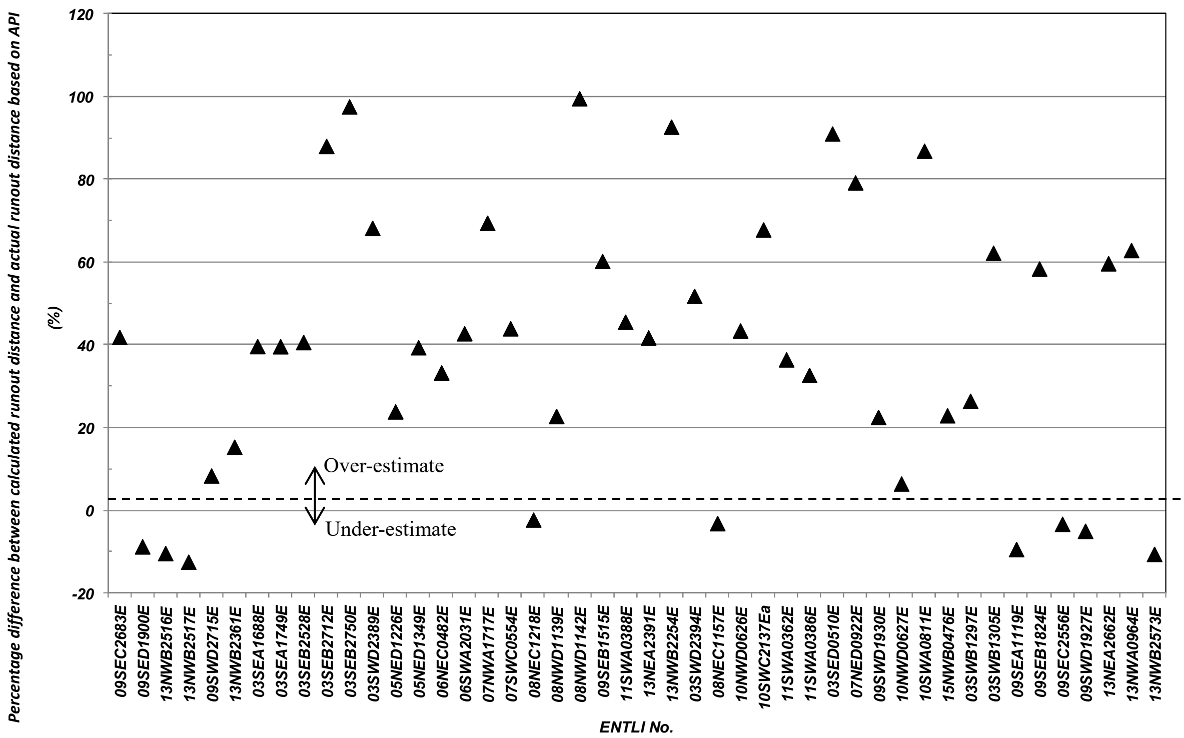

Note: $$\% \text{ difference in runout distance} = \frac{\text{(Calculated runout distance - Actual runout distance based on API)}}{\text{Actual runout distance based on API}} \times 100\%.$$

Figure 3.2 Estimation of Runout Distance Using $\phi_a = 18^{\circ}$, $\xi = 1000$ m/s^2

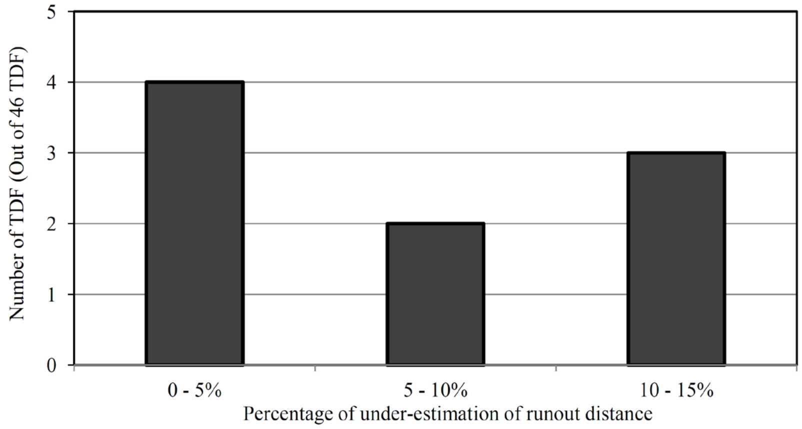

Figure 3.3 Under-estimation of Runout Distances Using ϕ_a = 18°, ξ = 1000 m/s^2

3.2 Benchmarking against the Kau Lung Hang Shan TDF

GEO (2006) documents an investigation of a natural terrain landslide in Kau Lung Hang Shan (ENTLI No. 03SWD2586E), in which super-elevation data observed on site and debris velocity estimated from the super-elevation data are reported. The landslide occurred in 2003 and was classified as a debris flow at that time. The reported source volume is about 200 m^3. Entrainment was assessed to be negligible. Figure 3.4 shows a general view of the landslide.

Re-interpretation of the landslide using aerial photographs conducted as part of this study has confirmed that the landslide occurred within a topographic depression. The reported runout distance of the landslide is some 160 m. Since this runout distance is less than 175 m, the landslide was not included in the identification exercise illustrated in Figure 2.1, and hence not selected for the mobility analyses reported in Section 3.1.

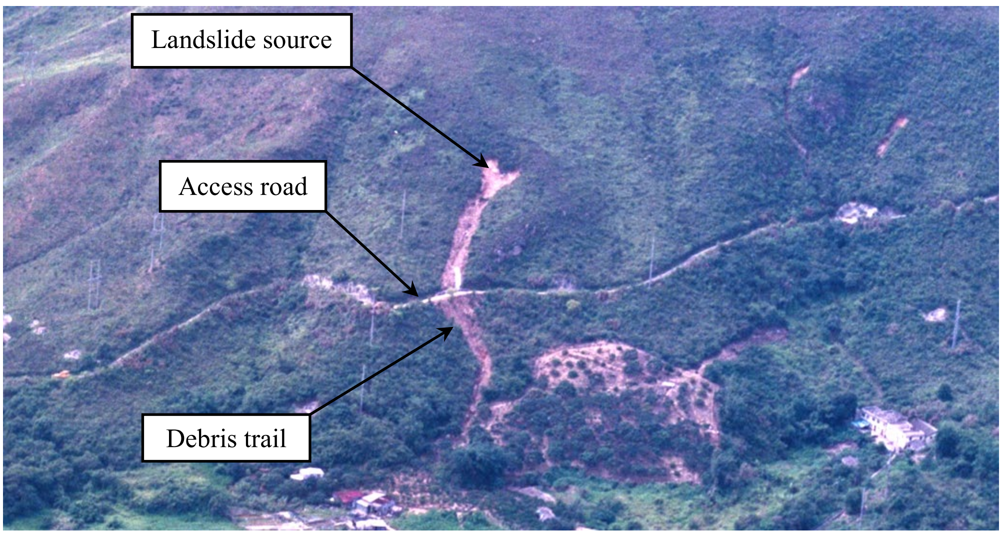

Figure 3.4 The Kau Lung Hang Shan Failure (GEO, 2006)

2d-DMM analysis which adopts rheological parameters 18°-1000 m/s^2 is benchmarked against the reported debris runout distance and the estimated velocities of the TDF at Kau Lung Hang Shan. The runout distance estimated by the analysis is 147 m, which is 10% lower than the reported value. The debris trail was intercepted by an access road. According to GEO (2006), a considerable amount of surface runoff from the access road could have been discharged into the landslide trail after the debris runout event, and actions of overland flow at the distal end of the debris trail were evident. Therefore, the extent of the debris deposition was probably affected and the actual runout distance could have been shorter than the reported value.

Figure 3.5 shows the velocity profile predicted by the mobility analysis. The debris velocities reported by GEO (2006) are presented for comparison. The debris velocity was estimated based on the super-elevations observed on site. At Chainage 66 (CH 66) and Chainage 73 (CH 73), the reported super-elevations were 2 m to 3 m. However, based on site photographs and field mapping records, there is no evidence of change in direction of debris travelling at these two locations. The locations of CH 66 and CH 73 were immediately below the access road on which a portion of debris was accumulated (see also Figure 3.4). The unconfined spreads of debris from the road were probably mistaken as super-elevations. Therefore, reported debris velocities at these two chainages were not included in Figure 3.5.

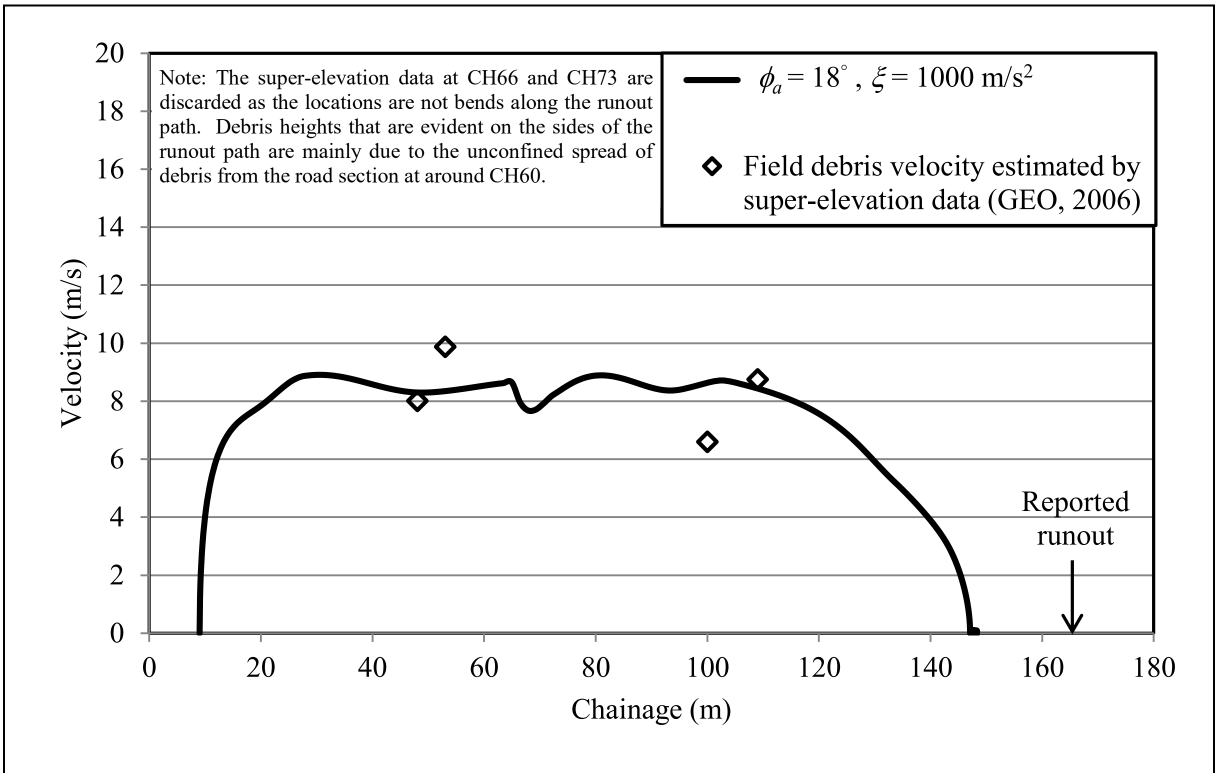

Figure 3.5 Calculated Debris Velocity Profile and Estimated Debris Velocities

Field measurements of super-elevation could not be made very precisely given the difficult site conditions and the fact that the debris trail could have been modified by surface water after the landslide event. However, the measurements could indicate the likely order of magnitude of the debris velocity. As noted from Figure 3.5, the mobility analysis using rheological parameters ϕ_a = 18° and ξ = 1000 m/s^2 provides a reasonable velocity estimate for the TDF at Kau Lung Hang Shan.

3.3 Effect of Source Volume

The source volumes of the 46 TDF studied range from 31 m^3 to 3,968 m^3 (see Figure 3.6). The volume dependence of the runout distance estimation has been examined. Figure 3.7 shows that the magnitudes of over-estimation/under-estimation do not correlate with the landslide source volume, which suggests that the use of different sets of rheological parameters for different landslide volumes would not be appropriate.

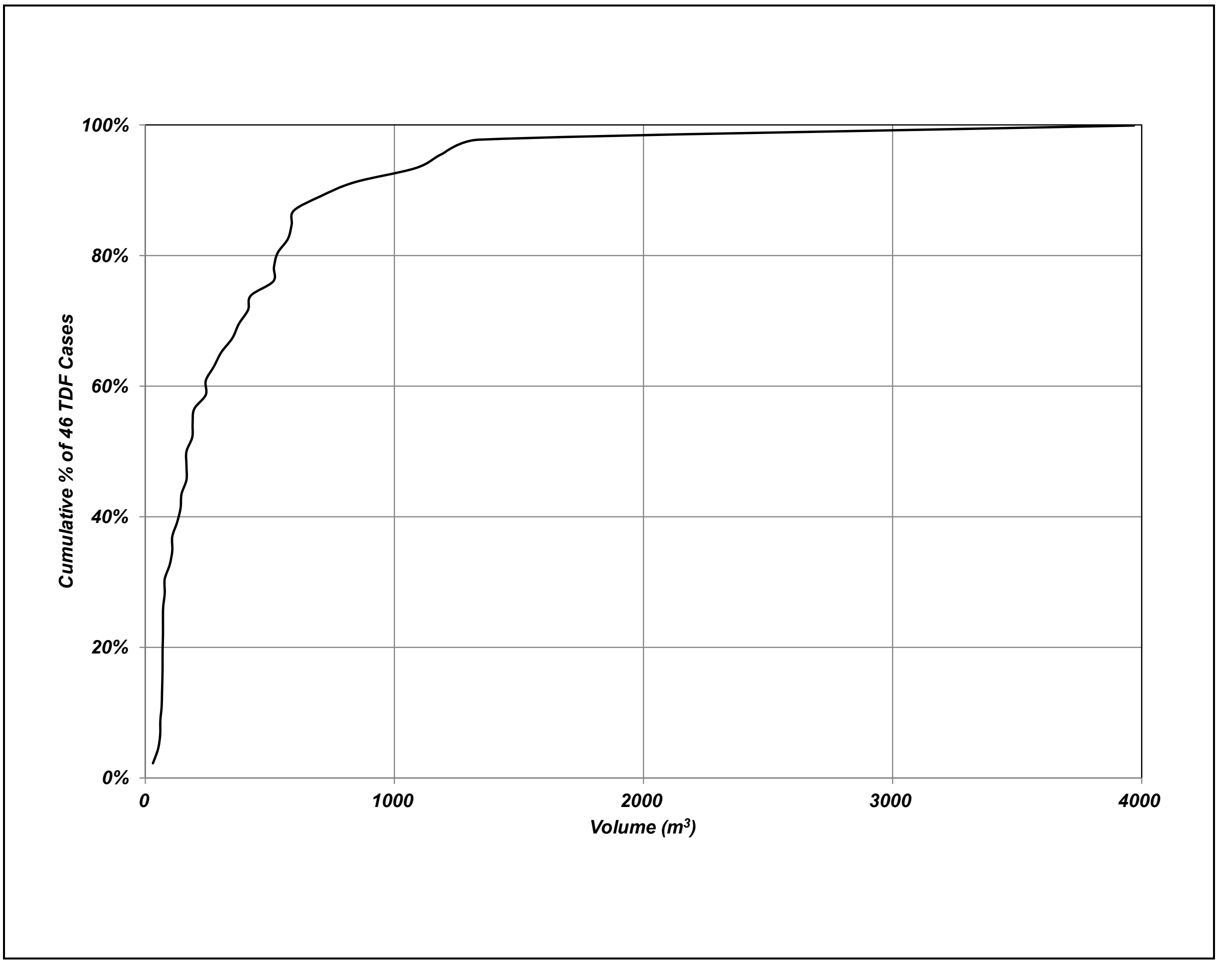

Figure 3.6 Cumulative Percentage of the 46 TDF in Terms of Source Volume

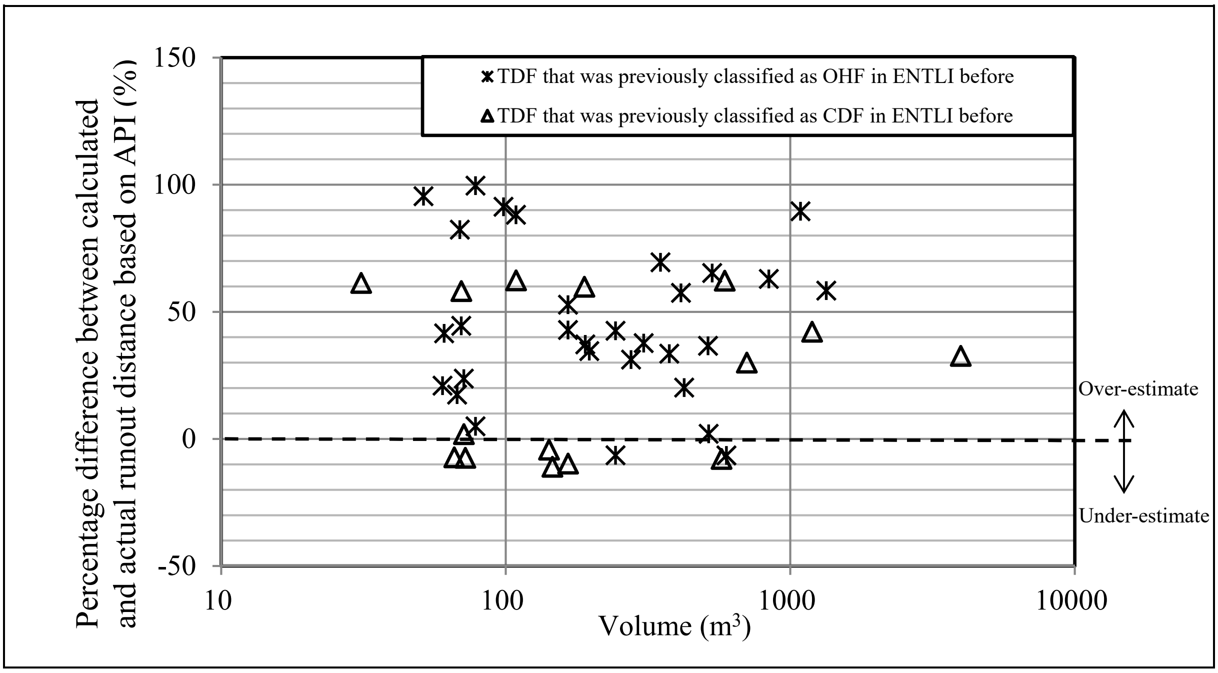

Figure 3.7 Runout Distances Estimated Using ϕ_a = 18°, ξ = 1000 m/s^2 According to Landslide Volumes

4 Discussion

Mobility analyses using Voellmy model with rheological parameter set of ϕ_a = 18° and ξ = 1000 m/s^2 do not over-estimate all the 46 mobile TDF. Where forward prediction of the mobility TDF is to be carried out, assessment as to whether the historical landslides in the TD catchment have resulted in more mobile debris runout than that assessed by the rheological parameter set 18°-1000 m/s^2 should be conducted.

2d-DMM was used for conducting the mobility analysis in the present study. Landslide debris is modelled as a homogeneous continuum material in the analysis. An explicit Lagrangian numerical scheme proposed by Hungr (1995) to solve the governing equations of unsteady non-uniform shallow water flow equations is adopted. Computer programs developed based on the same modelling technique or demonstrated to have performance similar to 2d-DMM can be used when rheological parameters recommended by this study are adopted for mobility assessment of TDF.

5 Conclusions and Recommendations

Historical mobile TDF were identified and mobility analyses of these mobile TDF were carried out. Mobility analyses using Voellmy parameters ϕ_a = 18° and ξ = 1000 m/s^2 produce suitably conservative estimates of runout distances of most of the mobile TDF, and velocities that match reasonably well with the field velocities deduced from a historical TDF in Kau Lung Hang Shan. It is considered that the rheological parameters could be adopted for forward prediction purposes. However, due regard should be given to assessing whether the historical landslides in the TD catchments of concern have resulted in more mobile debris runout than that assessed by the recommended rheological parameters.

Based on the results of the study, technical recommendations are given as follows:

(a) Voellmy model should be used for the assessment of debris mobility of TDF. Except for situations referred to in the paragraph below, the generic rheological parameters that should be used are $\phi_a = 18^o$ and $\xi = 1000$ m/s^2; and

(b) where historical landslides in the TD catchments have resulted in more mobile debris runout than that assessed using the above recommended rheological parameters, the appropriate rheological parameters to be adopted in analytical design of TDF mitigation measures should be assessed on a case-by-case basis, with account taken of the back-analysed rheological parameters of the historical TDF within the TD catchments of concern and any other relevant factors that may affect debris mobility.

6 References

GEO (2006). *The 5 May 2003 Debris Flow at Kau Lung Hang Shan, Tai Po (GEO Report No. 196)*. Geotechnical Engineering Office, Hong Kong, 84 p.

GEO (2011). *Guidelines on the Assessment of Debris Mobility for Channelized Debris Flows (TGN No. 29).* Geotechnical Engineering Office, Hong Kong, 6 p.

GEO (2012a). *Guidelines on the Assessment of Debris Mobility for Open Hillslope Failures (TGN No. 34).* Geotechnical Engineering Office, Hong Kong, 16 p.

GEO (2012b). *User Manual for Computer Program "2d-DMM" - Two-dimensional Debris Mobility Model (Spreadsheet Version 1.2).* Geotechnical Engineering Office, Hong Kong, 58 p.

GEO (2013). *Guidelines on Enhanced Approach for Natural Terrain Hazard Studies under LPMitP (TGN No. 36).* Geotechnical Engineering Office, Hong Kong, 18 p.

Hungr, O. (1995). A model for the runout analysis of rapid flow slides, debris flows and avalanches. *Canadian Geotechnical Journal*, vol. 32, pp 610-623.

Lo, D.O.K. (2000). *Review of Natural Terrain Landslide Debris-resisting Barrier Design (GEO Report No. 104)*. Geotechnical Engineering Office, Hong Kong, 91 p.

Ng, K.C., Parry, S., King, J.P., Franks, C.A.M. & Shaw, R. (2003). *Guidelines on Natural Terrain Hazard Studies (GEO Report No. 138).* Geotechnical Engineering Office, Hong Kong, 138 p.

Pudasaini, S.P. & Hutter, K. (2007). *Avalanche Dynamics*. Springer, 602 p.

Tattersall, J.W., Devonald, D.M., Hung, R.K.C. & Kwong, R.T.S. (2009). Estimation of 'design event' landslide sources for the North Lantau Expressway and Yu Tung Road natural terrain hazard mitigation works study. *Proceedings of the 2009 Hong Kong Institution of Engineers Geotechnical Division Annual Seminar*, Geotechnical Division, HKIE, pp 141-147.

Wong, H.N., Ko, F.W.Y. & Hui, T.H.H. (2006). *Assessment of Landslide Risk of Natural Hillsides in Hong Kong (GEO Report No. 191)*. Geotechnical Engineering Office, Hong Kong, 117 p.

Appendix A

Classification of Hillside Catchments Extracted from GEO TGN 36

Content

	Page No.
List of Table	22

List of Table

Table No.		Page No.
A1	Classification of Hillside Catchments	23

Table A1 Classification of Hillside Catchments (Sheet 1 of 2)

Catchment Characteristics	Channelised (CD) Catchment	Topographic Depression (TD) Catchment	Open Hillslope (OH) Catchment
Topography	• Presence of an incised drainage channel. • In practice, this applies to catchments with the presence of a well-defined drainage channel based on the contours or a hydro-line feature shown in the Land Information Centre (LIC) 1:1,000-scale topographic map, unless otherwise invalidated by aerial photograph interpretation, airborne LiDAR data, information from historical landslides, and/or field mapping. • The degree of confinement provided by the drainage line should be considered in relation to the design event being considered.	• Presence of a pronounced topographic depression but without a well-defined drainage channel. • In practice, this applies to catchments without the presence of a hydro-line feature in the LIC 1:1,000-scale topographic map but where a certain degree of confinement can be observed based on the contours of the LIC 1:1,000-scale topographic map, and where debris would converge and travel downslope. This should be verified by aerial photograph interpretation, airborne LiDAR data, information from historical landslides, and/or field mapping. • The topographic depression can vary from well defined valleys of limited extent to linear depressions on otherwise planar slopes. • In general, the plan distance between the downslope end of the topographic depression and the facilities at risk would normally be less than 100 m.	• Generally planar slope as observed from the LIC 1:1,000-scale topographic map, with neither a conspicuous drainage channel nor pronounced topographic depression. This should be verified by aerial photograph interpretation, airborne LiDAR data, information from historical landslides, and/or field mapping.
Drainage/Debris Concentration	• Has a high drainage concentration in general, i.e. the section through which debris would be discharged is significantly small compared with that of its upstream catchment.	• Has some drainage concentration in general, i.e. the section through which debris would be discharged is relatively small compared with that of its upstream catchment. There is evidence of only limited surface water flow occurring and only in significant rainstorms.	• Has insignificant drainage concentration, i.e. the width of the section through which debris would be discharged is comparable to (or even greater than) that of its source area width or upstream catchment.

Table A1 Classification of Hillside Catchments (Sheet 2 of 2)

Catchment Characteristics	Channelised (CD) Catchment	Topographic Depression (TD) Catchment	Open Hillslope (OH) Catchment
Discharge Outlet	• Debris from different sources within the catchment would travel downstream, given sufficient mobility, to a predictable discharge point.	• Debris would likely converge, given sufficient mobility, to a likely discharge point, i.e. debris would continue to travel along a preferential pathway until exiting the topographic depression at or near the site boundary.	• Debris from different sources within the catchment could travel downslope, given sufficient mobility, to different discharge points and may involve the lateral spreading of debris.
Debris Path	• Debris path is controlled by the alignment and confinement of the drainage line. • 'Overshooting' of debris laterally from the drainage line is very unlikely within the main drainage line. However, near the exit point or where a debris fan is present this may occur.	• Debris path is somewhat confined by topography and may either be curved or relatively straight. • Possibility of 'overshooting' of debris laterally from the topographic depression is unlikely but cannot be excluded entirely, depending on the size of the potential failure event relative to the dimensions of the depression.	• Debris path is relatively unconfined, straight, and tends to follow the line of greatest slope which has insignificant change in its dip direction. • Actual debris path may be different from that assessed based on the line of greatest slope, e.g. due to uncertainty in the strike of the failure plane at source and resolution of the available data.
Potential Hazard to Consider	• Channelised debris flow (CDF) hazards. • High entrainment potential in general, dependent on presence of entrainable materials within the stream bed, the steepness and/or stability of channel sides.	• Debris flow (DF) hazards. • Lower entrainment potential than CDF in general, largely dependent on the steepness and presence of entrainable materials within the topographic depression.	• Open hillslope landslide (OHL) hazards (i.e. debris slide or debris avalanche on a relatively planar slope). • No entrainment potential in general.

Notes:

(1) It should be noted that the potential hazard of a small CD catchment may be more akin to a TD catchment and hence in such cases a small CD catchment may be treated as a TD catchment. Similarly, the potential hazard of a small TD catchment may be more akin to an OH catchment and hence in such cases a small TD catchment may be treated as an OH catchment. In these cases, judgement needs to be exercised and justifications should be provided.

(2) The possibility of presence of localised topographic depression on an OH catchment and affecting debris movement mechanism cannot be excluded, e.g. due to the hillslope being not entirely planar, resolution of the available data, and local concavity due to gully erosion and landsliding.

Appendix B

List of Mobile Failures within Topographic Depression Catchments Identified in ENTLI

Content

	Page No.
List of Table	27

List of Table

Table No.		Page No.
B1	List of Mobile Failures within Topographic Depressions Identified in ENTLI	28

Table B1   List of Mobile Failures within Topographic Depressions Identified in ENTLI

ENTLI No.	Source Length (m)	Source Width (m)	Aerial Photograph Year	Aerial Photograph No.	Runout Distance# (m)
03SEA1688E	11	12	1945	Y913-14	108
03SEA1749E	14	15	1963	Y9882-83	113
03SEB2528E	7	9.5	1988	A15017-18	114
03SEB2712E	9	10	1997	CN19240	122
03SEB2750E	6	9	2003	CW53911-12	113
03SED0510E	7	12	2003	CW48319-20	114
03SWB1297E	10.5	12.5	1993	CN5475-76	235
03SWB1305E	10	9	1993	CN5476-77	176
03SWD2389E	14	19	1993	CN5475-76	137
03SWD2394E	10	12	1993	CN5521-22	155
05NED1226E	7.5	9	2000	CN26601-02	127
05NED1349E	13.5	10	2000	CN26603-04	105
06NEC0482E	20	8.5	1949	Y1903-04	155
06SWA2031E	11	5.5	1982	44602-03	108
07NED0922E	12	5.5	1945	Y745-46	134
07NWA1717E	20	25	1999	CN24486-87	117
07SWC0554E	12	10	1997	CN19028-29	119
08NEC1157E	16	18	1963	Y10382-83	168
08NEC1218E	12	13	1981	39226-27	150
08NWD1139E	10	6.5	1978	24566-67	103
08NWD1142E	8	9	1978	24566-67	109
09SEA1119E	9	12	2008	CS20016-17	191
09SEB1515E	16	14	1992	CN3333-34	110
09SEB1824E	7	9.5	2008	CS19668-69	176
09SEC2556E	7.5	9	2008	CS14002-03	179
09SEC2683E	21	22	2008	CS14365-66	259
09SED1900E	8	8.5	2008	CS20175-76	213
09SWD1927E	20	14	1973	3932-33	194
09SWD1930E	10	6	1973	3932-33	101
09SWD2715E	18	14.5	2008	CS14896-97	135
10NWD0626E	12	13	1999	CN24215-16	154
10NWD0627E	9	8	1999	CN24215-16	116
10SWA0811E	25	8	1994	CN6127-28	100
10SWC2137Ea	52	7	1999	CN24291-92	173
11SWA0362E	30	35	1967	Y13297-98	252
11SWA0386E	23	14	1967	Y13299-300	236
11SWA0388E	20	13	1967	Y13299-300	119
13NEA2391E	13.5	13.5	1993	CN5278-79	134
13NEA2662E	4.5	8.5	2008	CS14036-37	175
13NWA0964E	19	15	1982	44807-08	181
13NWB2254E	25.5	17	1993	CN5238-39	116
13NWB2361E	11	8.5	2007	CW80034-35	129
13NWB2516E	8	8	2008	CS14393-94	317
13NWB2517E	10	12	2008	CS14393-94	275
13NWB2573E	10	11	2008	CS14391-92	186
15NWB0476E	19	12	1973	1690-91	114

Note: #The runout distance was estimated from the aerial photographs by this study.

Appendix C

Topographic Plans of Mobile Failures within Topographic Depression Catchments Identified in ENTLI

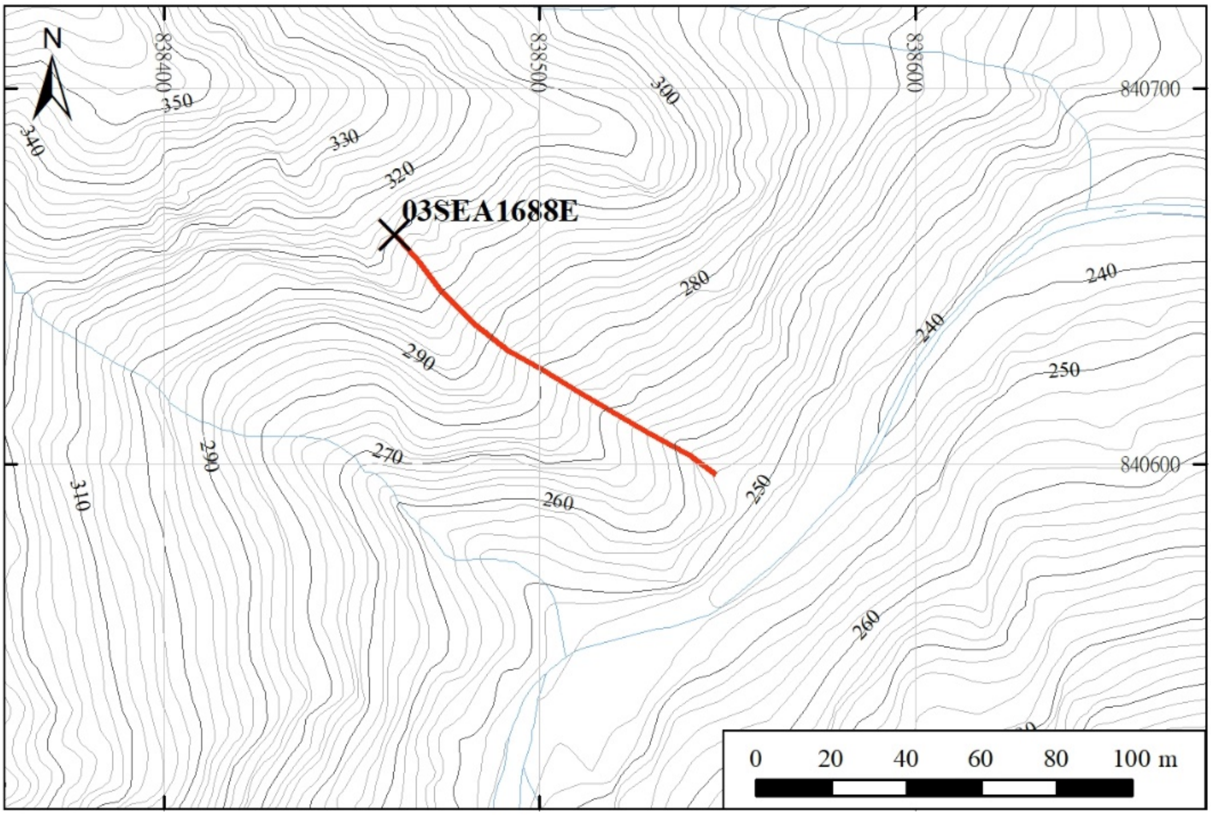

Location Plan of ENTLI No. 03SEA1688E

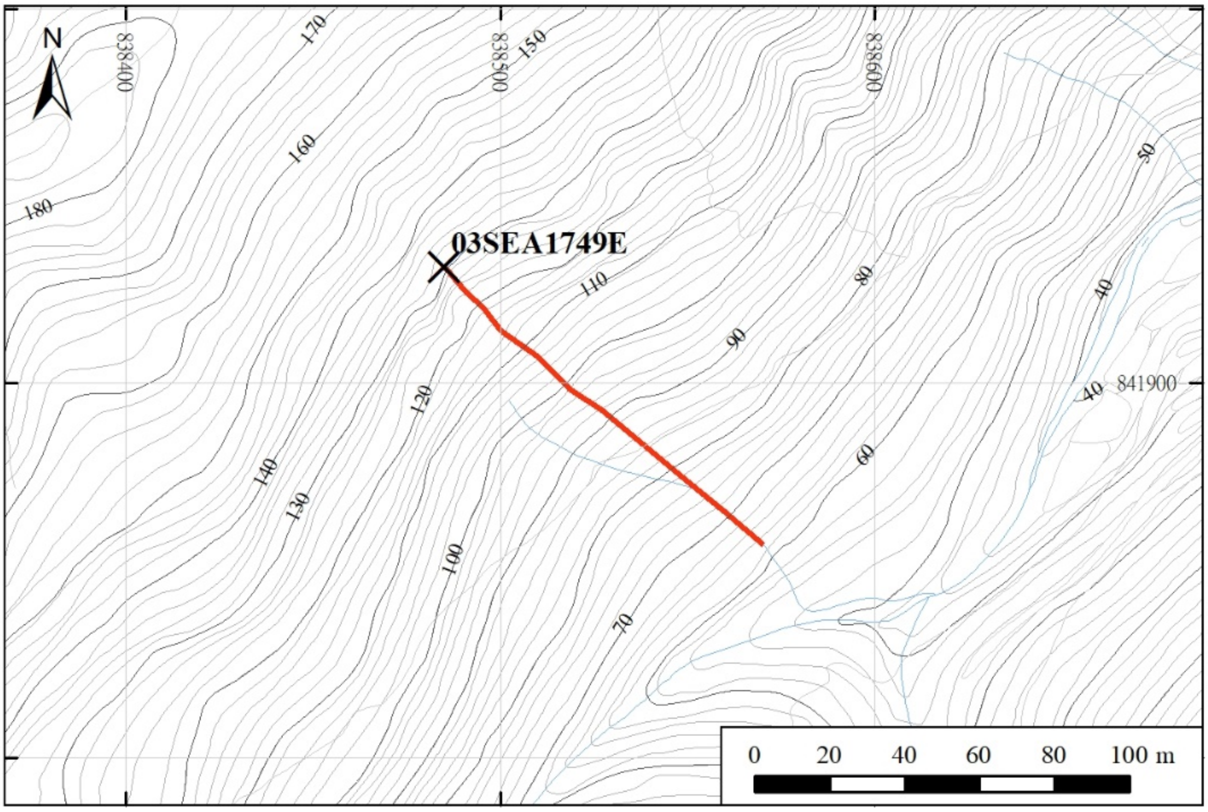

Location Plan of ENTLI No. 03SEA1749E

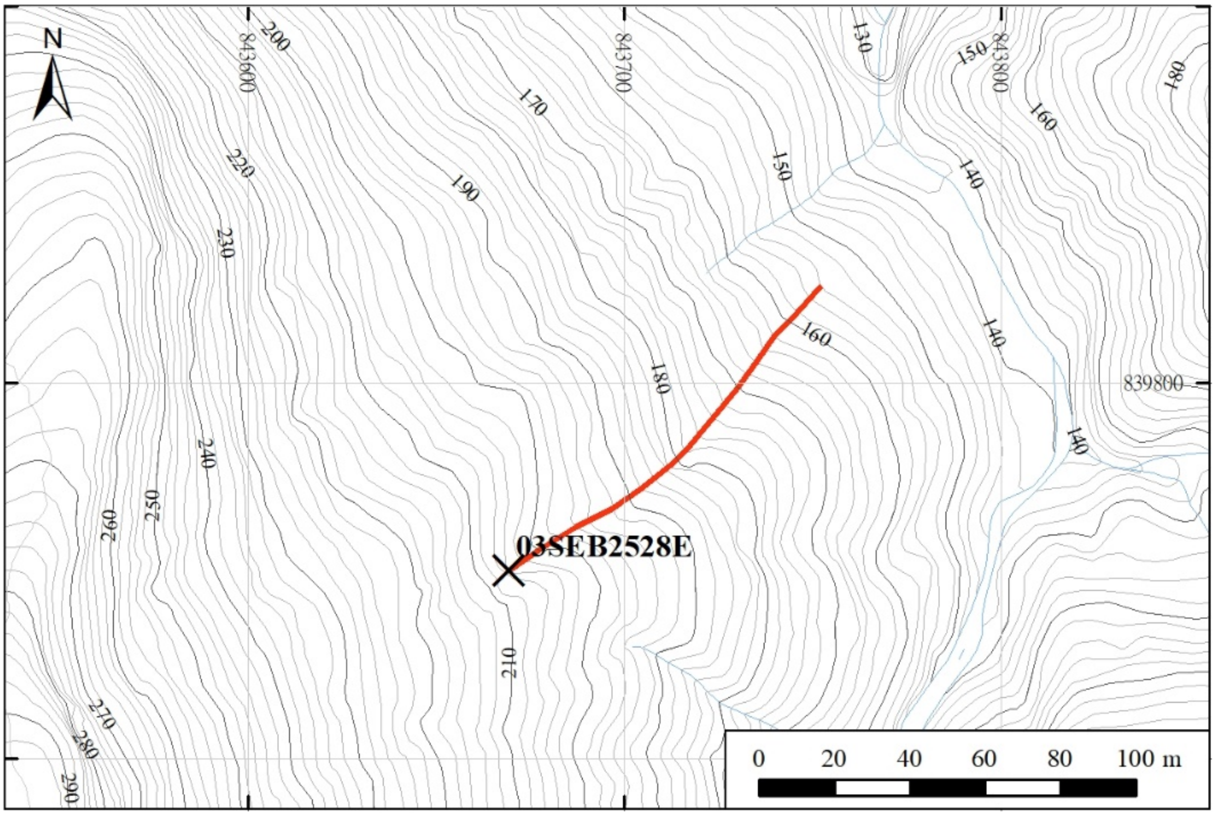

Location Plan of ENTLI No. 03SEB2528E

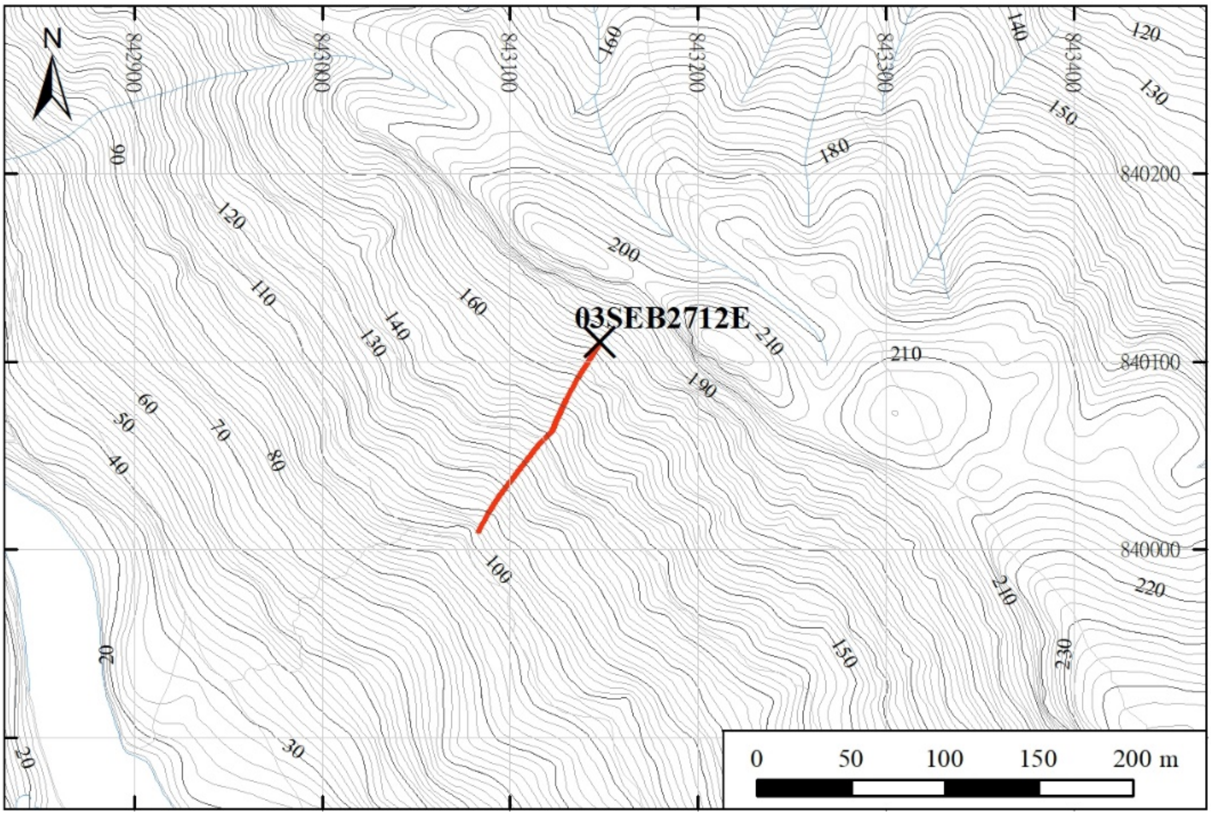

Location Plan of ENTLI No. 03SEB2712E

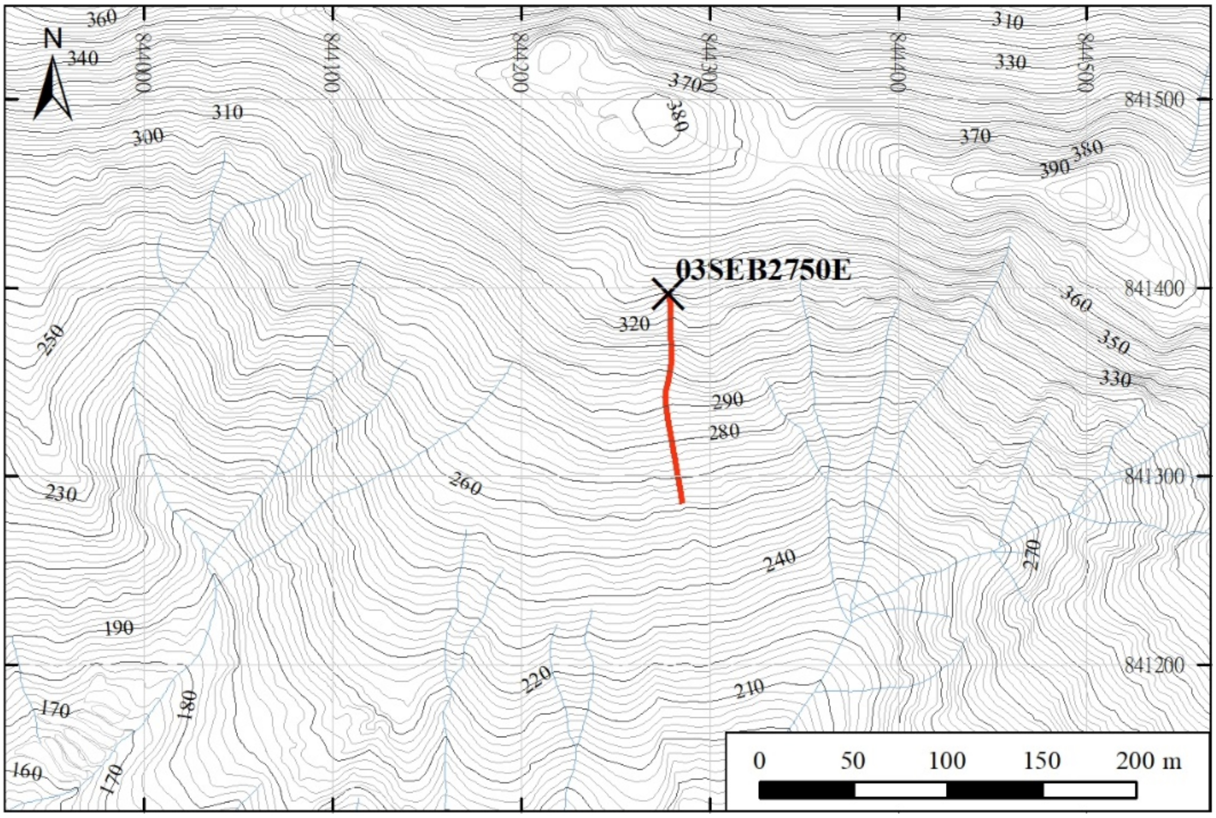

Location Plan of ENTLI No. 03SEB2750E

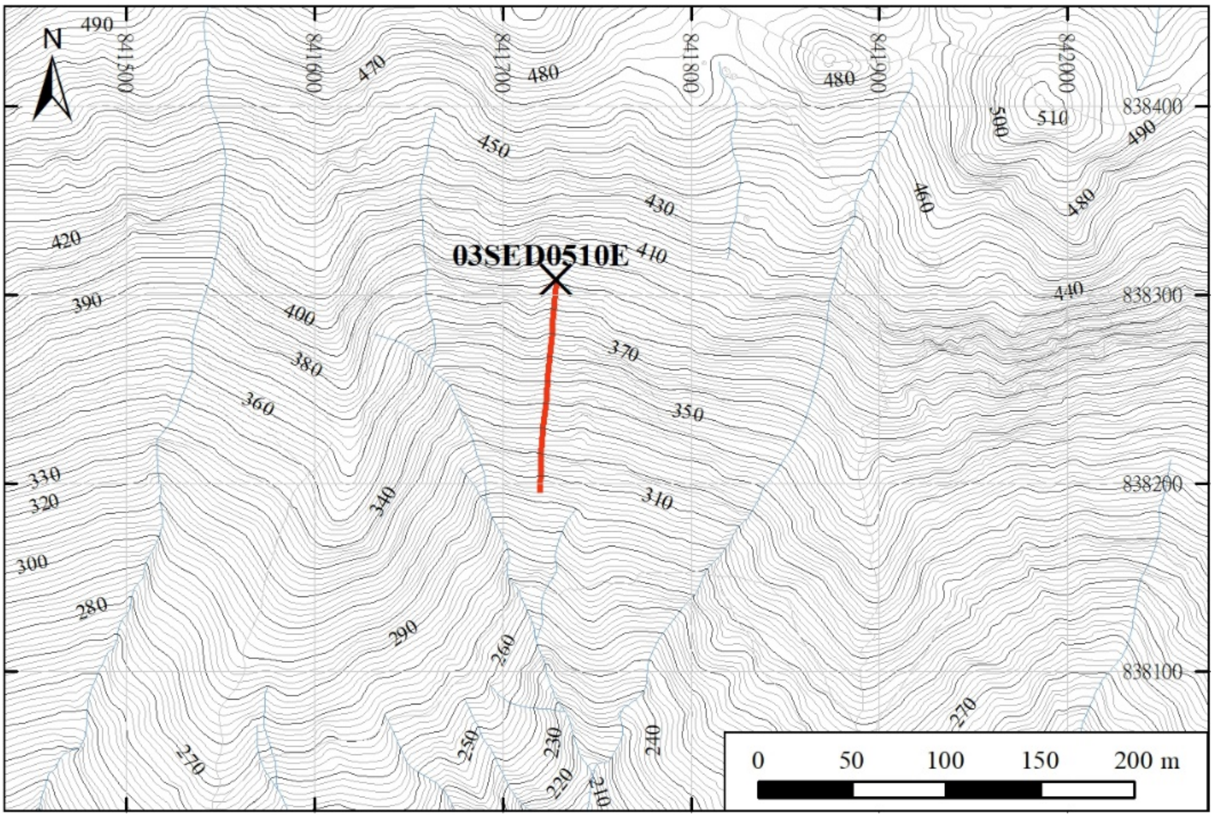

Location Plan of ENTLI No. 03SED0510E

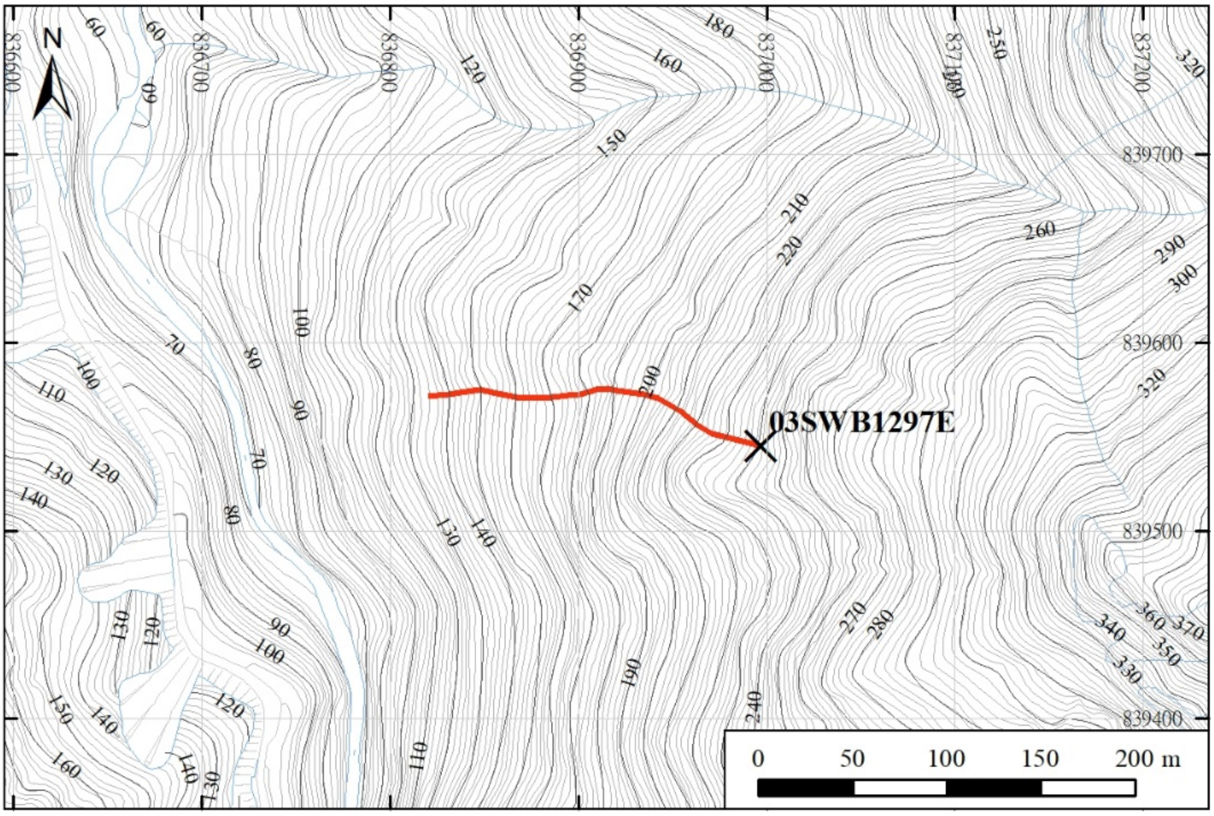

Location Plan of ENTLI No. 03SWB1297E

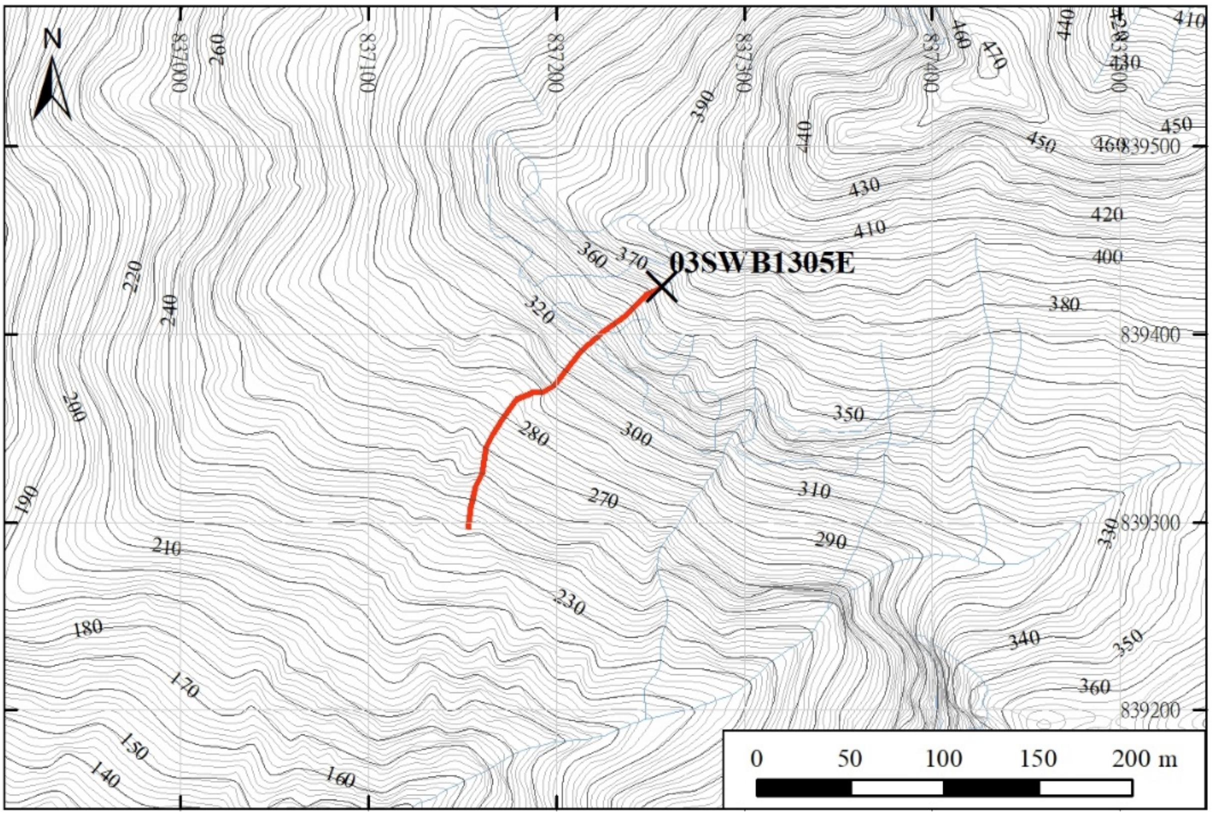

Location Plan of ENTLI No. 03SWB1305E

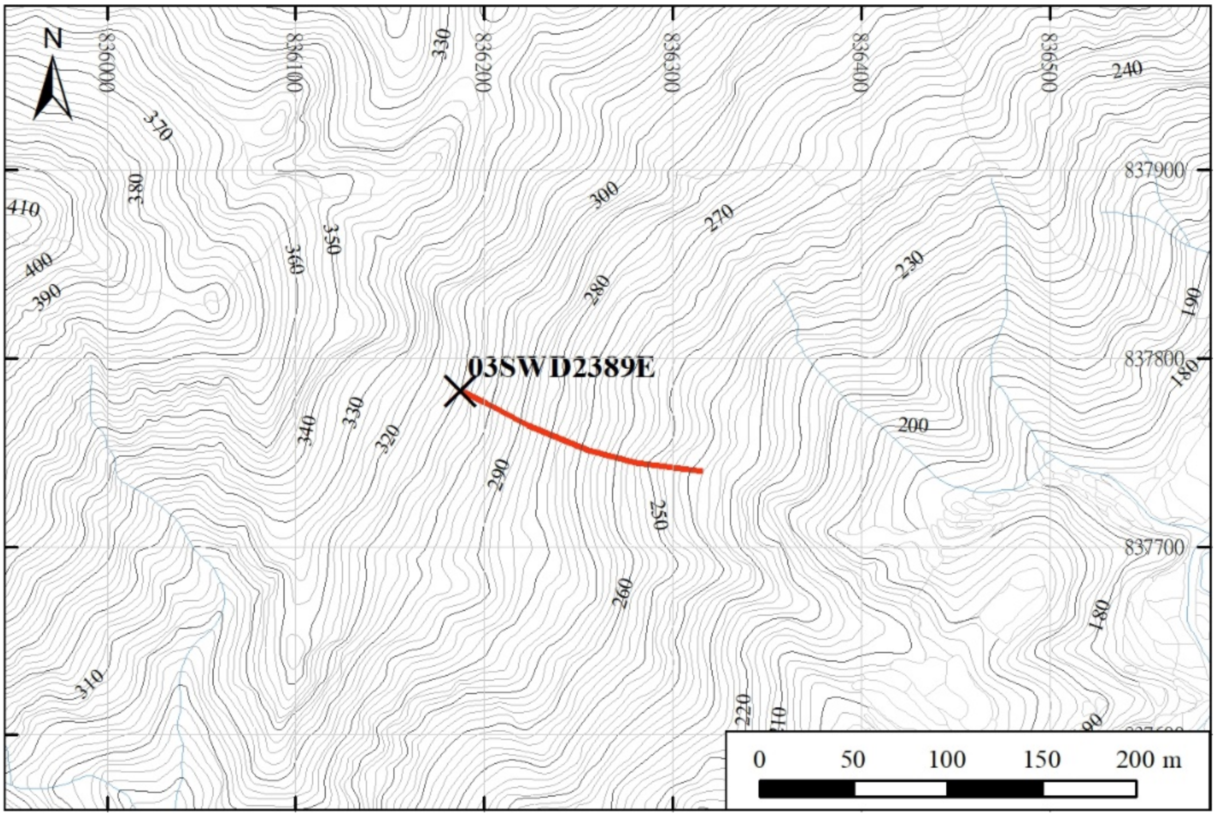

Location Plan of ENTLI No. 03SWD2389E

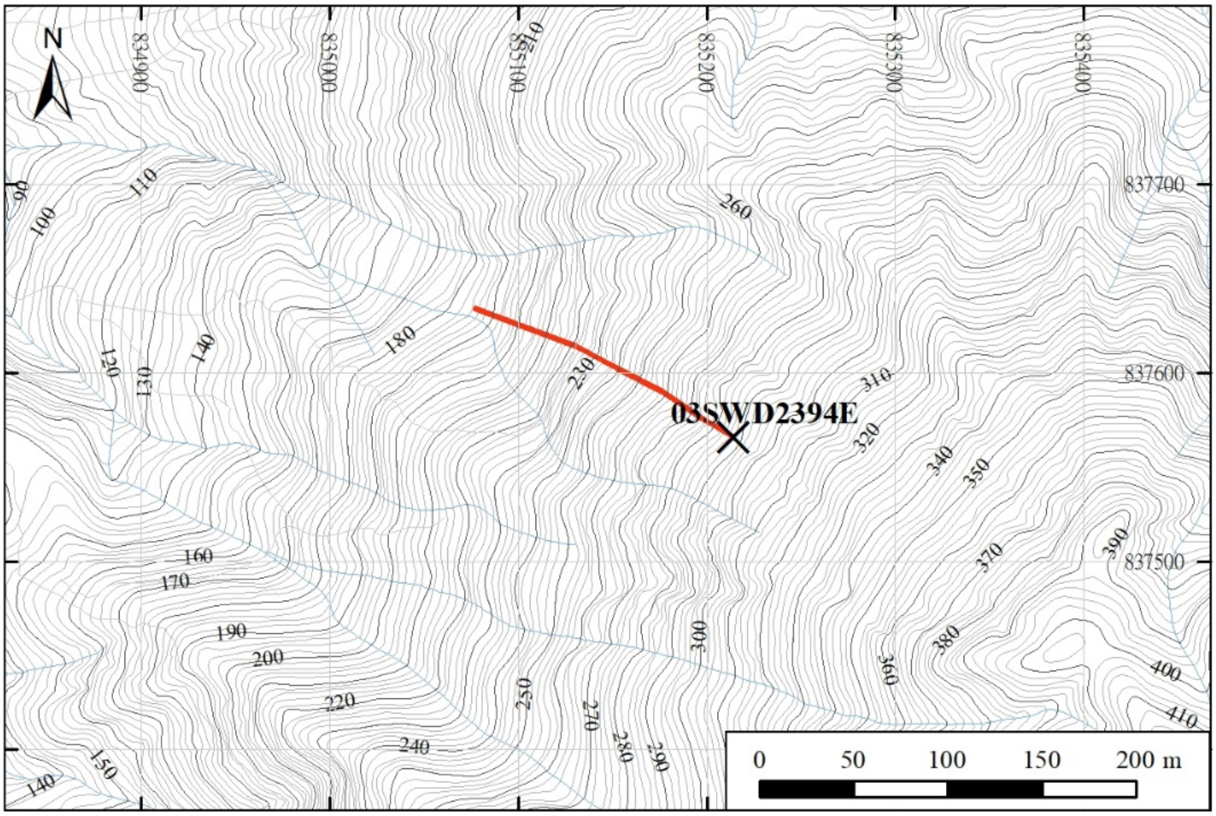

Location Plan of ENTLI No. 03SWD2394E

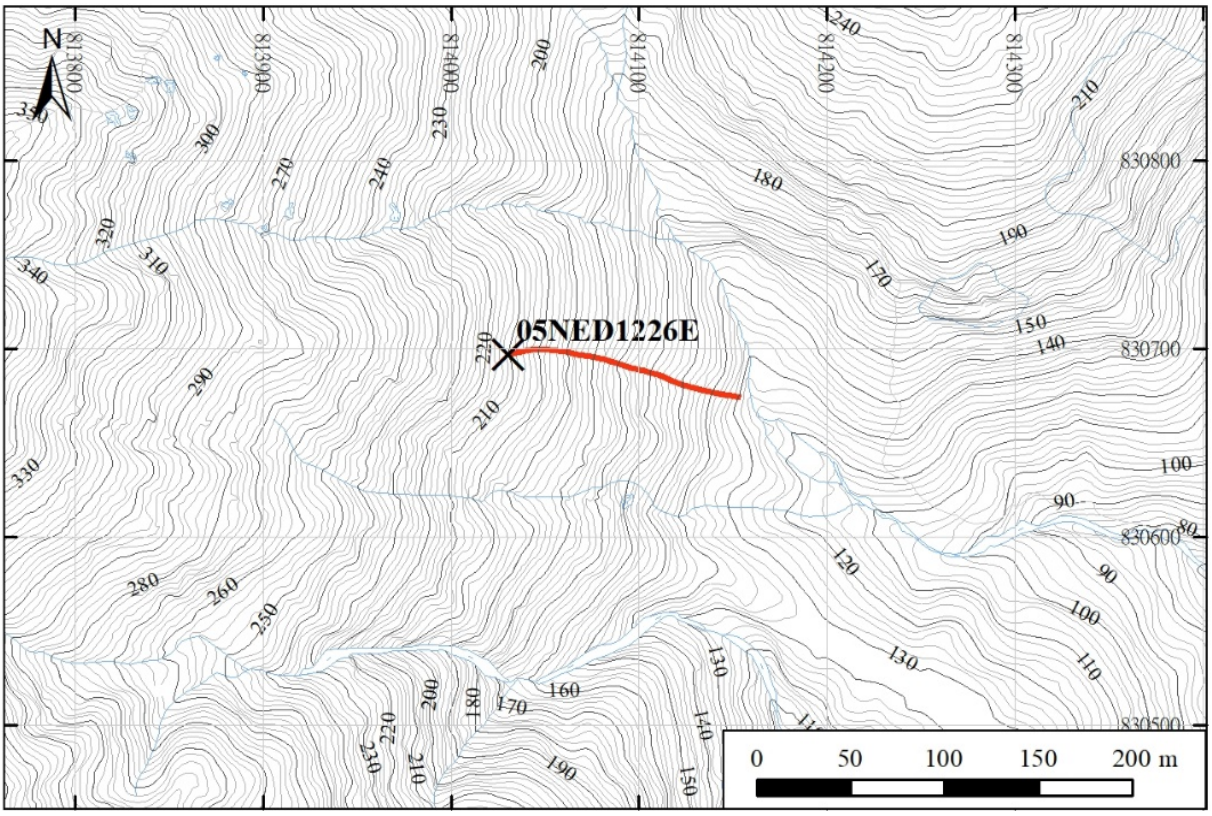

Location Plan of ENTLI No. 05NED1226E

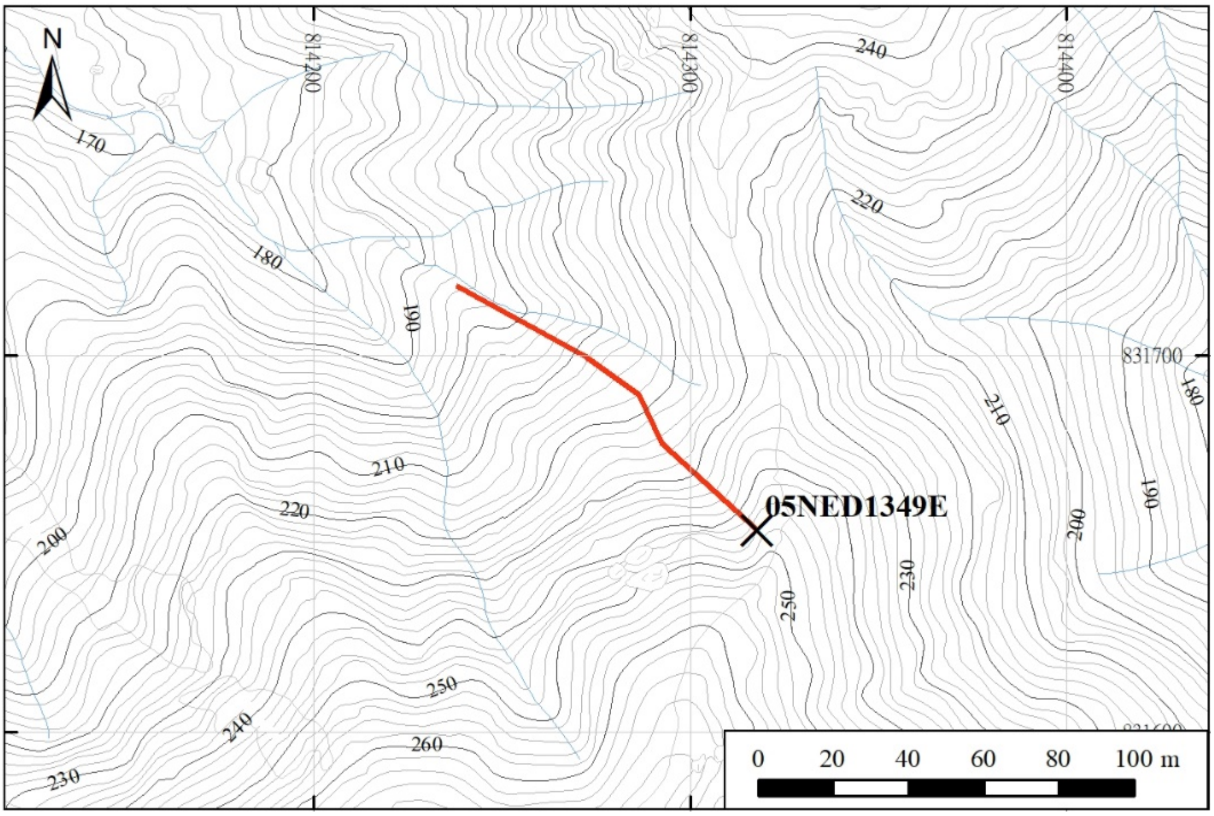

Location Plan of ENTLI No. 05NED1349E

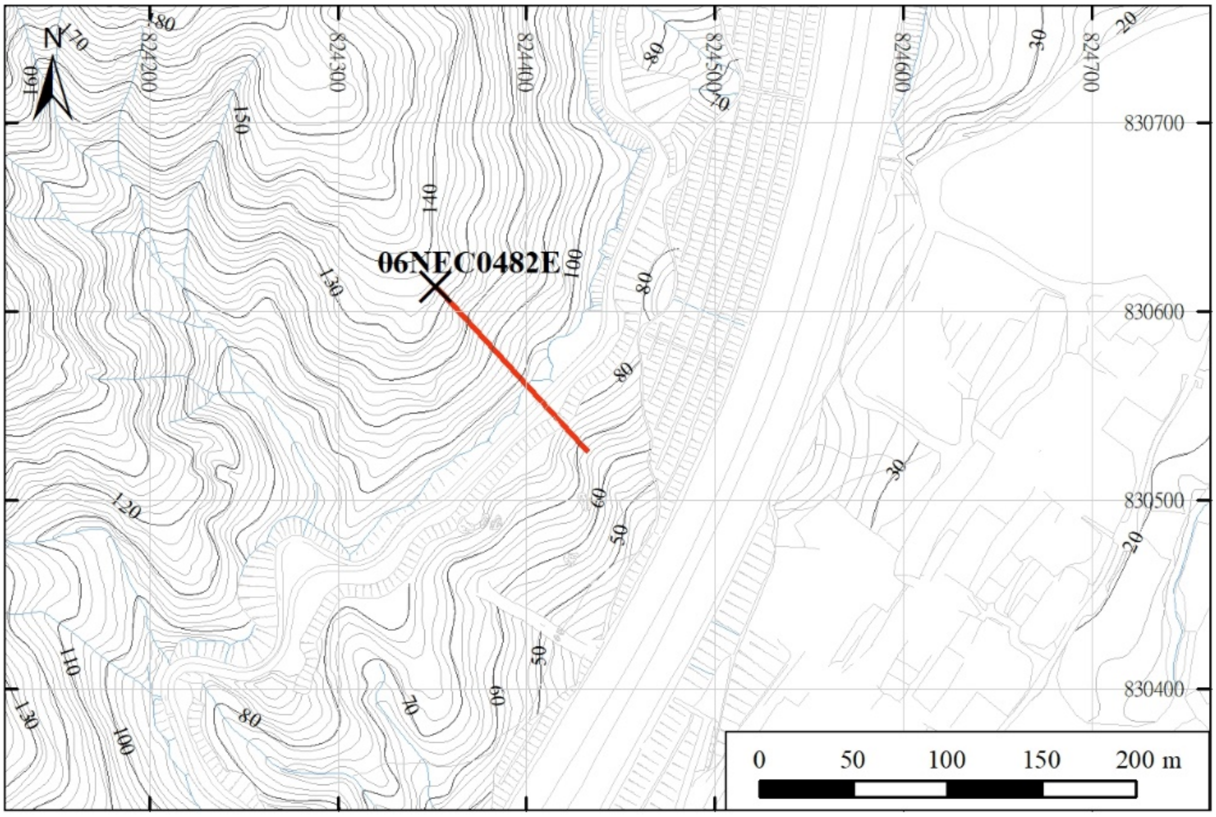

Location Plan of ENTLI No. 06NEC0482E

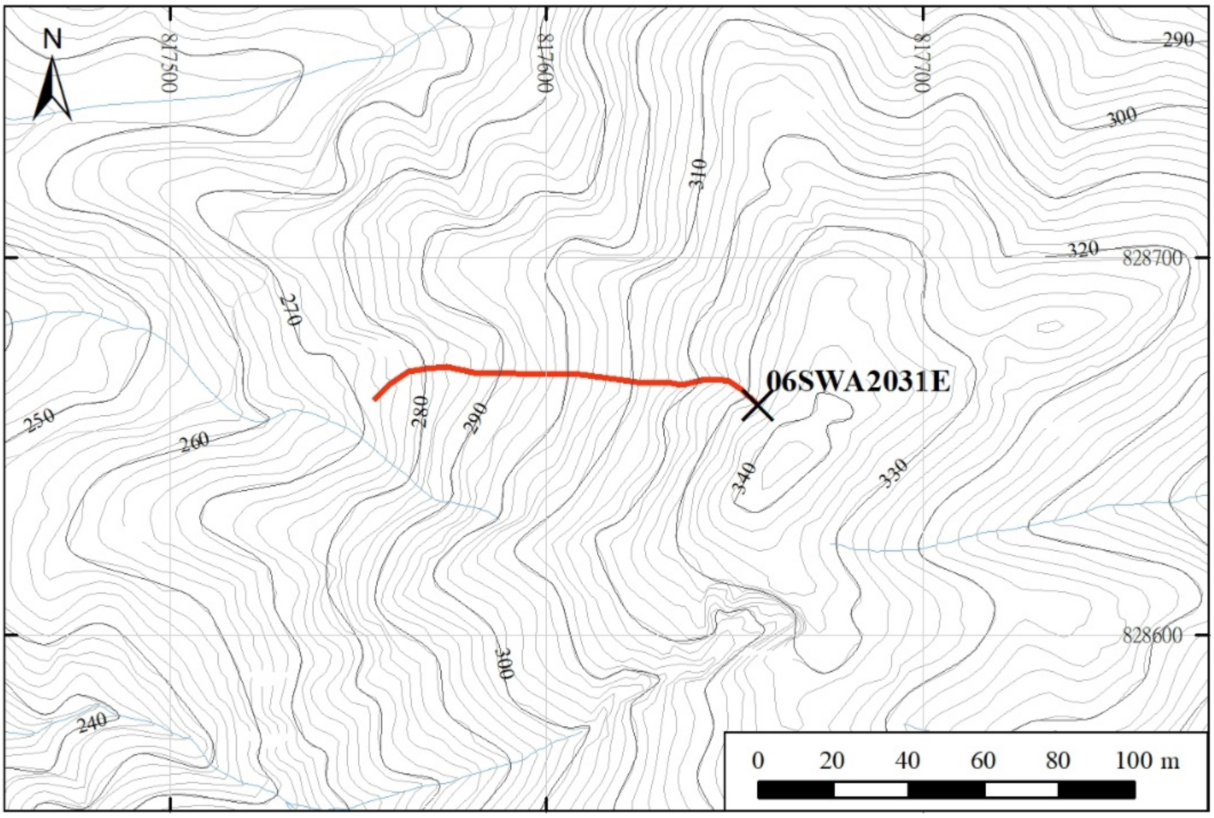

Location Plan of ENTLI No. 06SWA2031E

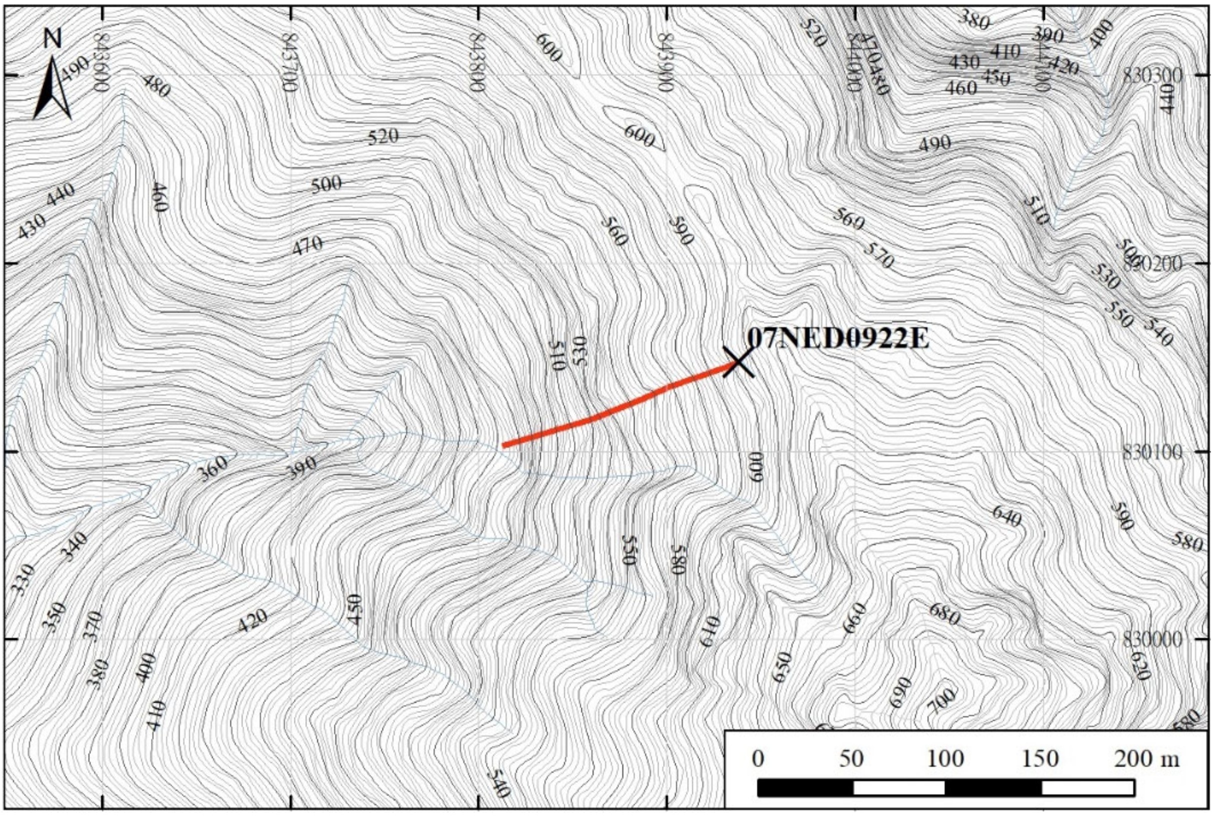

Location Plan of ENTLI No. 07NED0922E

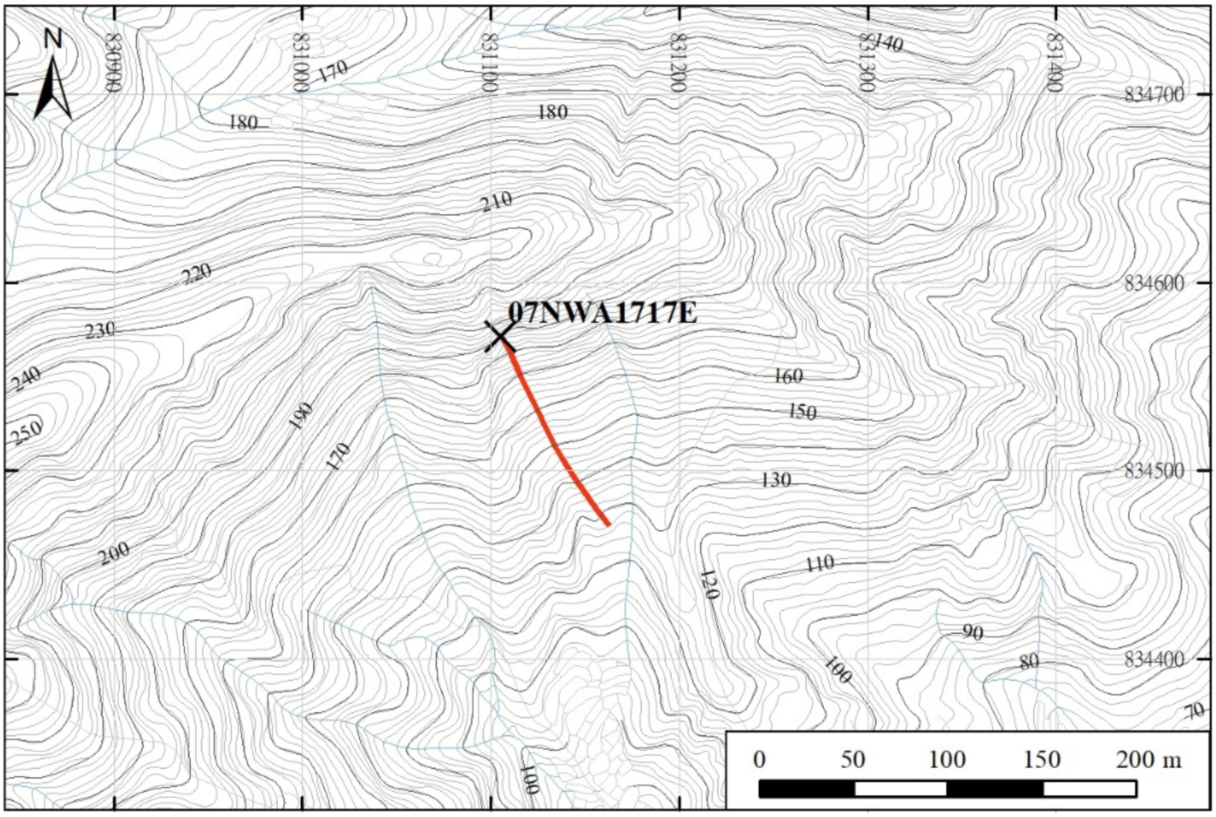

Location Plan of ENTLI No. 07NWA1717E

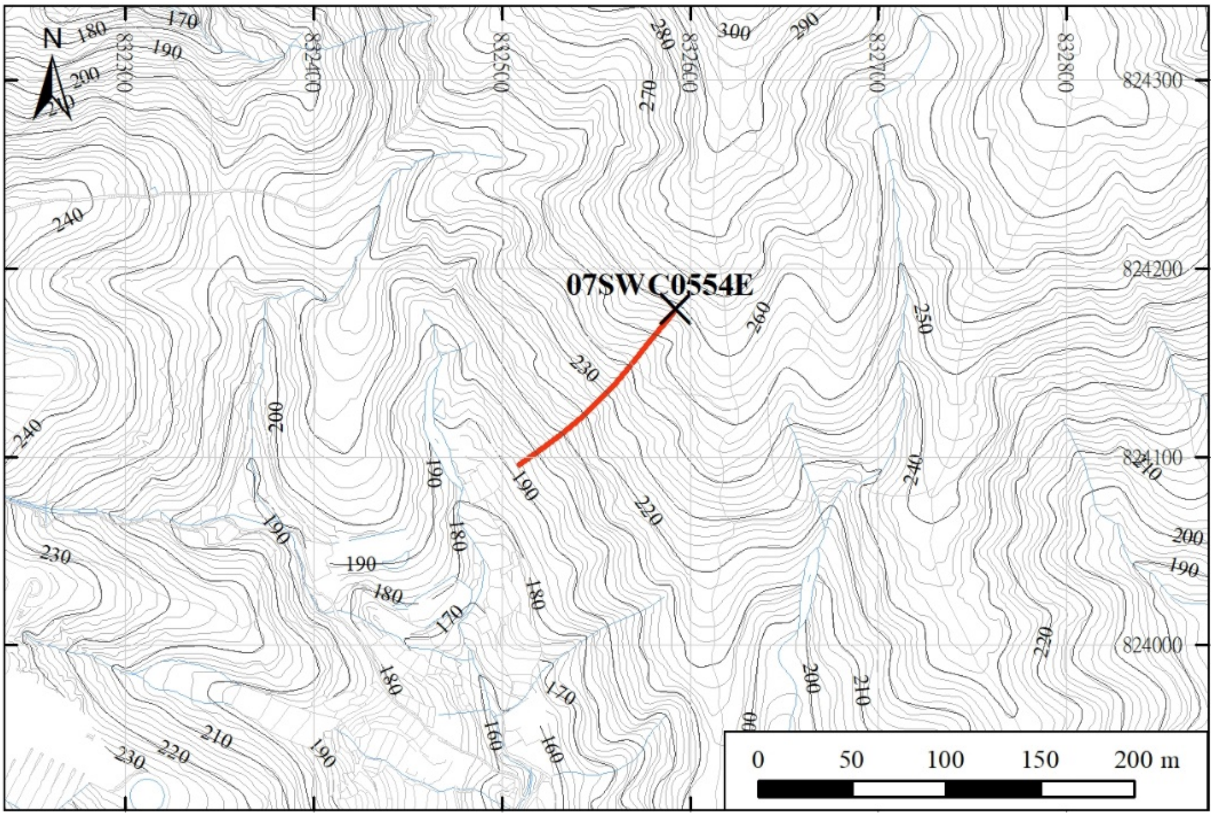

Location Plan of ENTLI No. 07SWC0554E

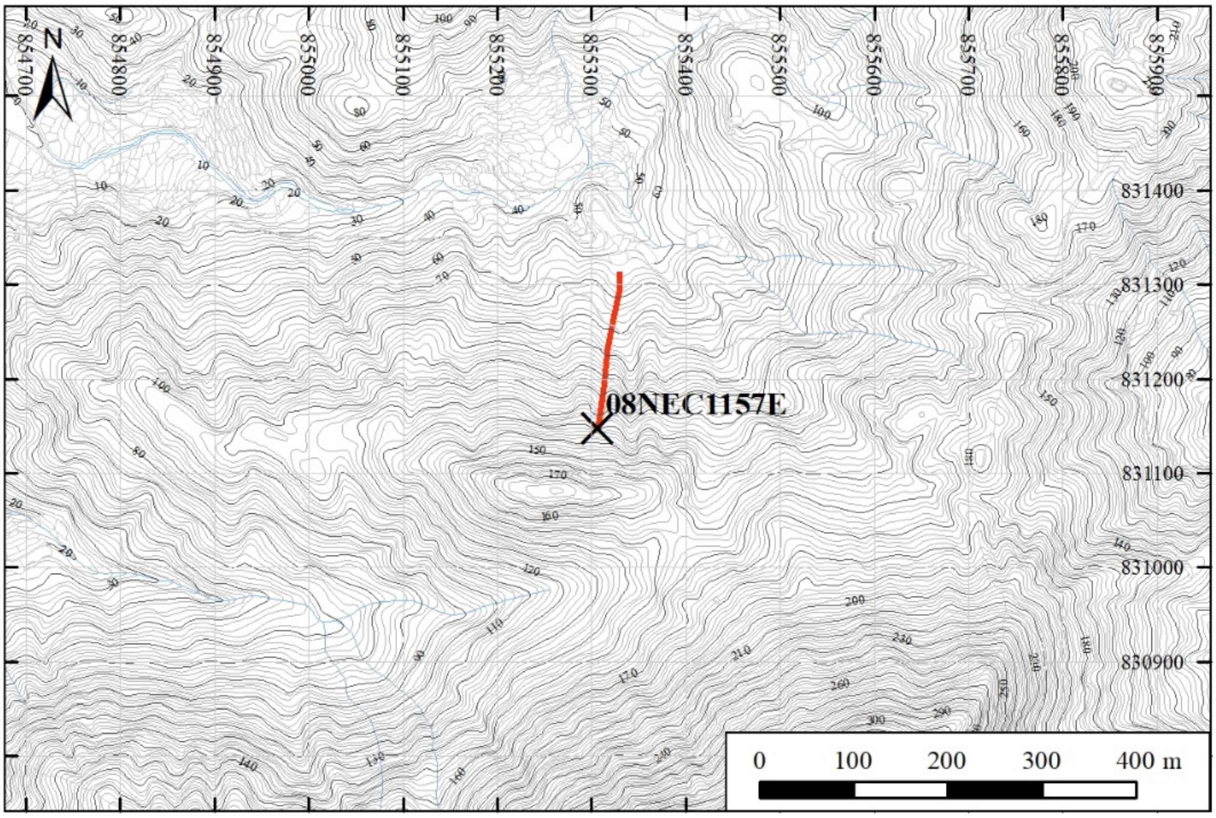

Location Plan of ENTLI No. 08NEC1157E

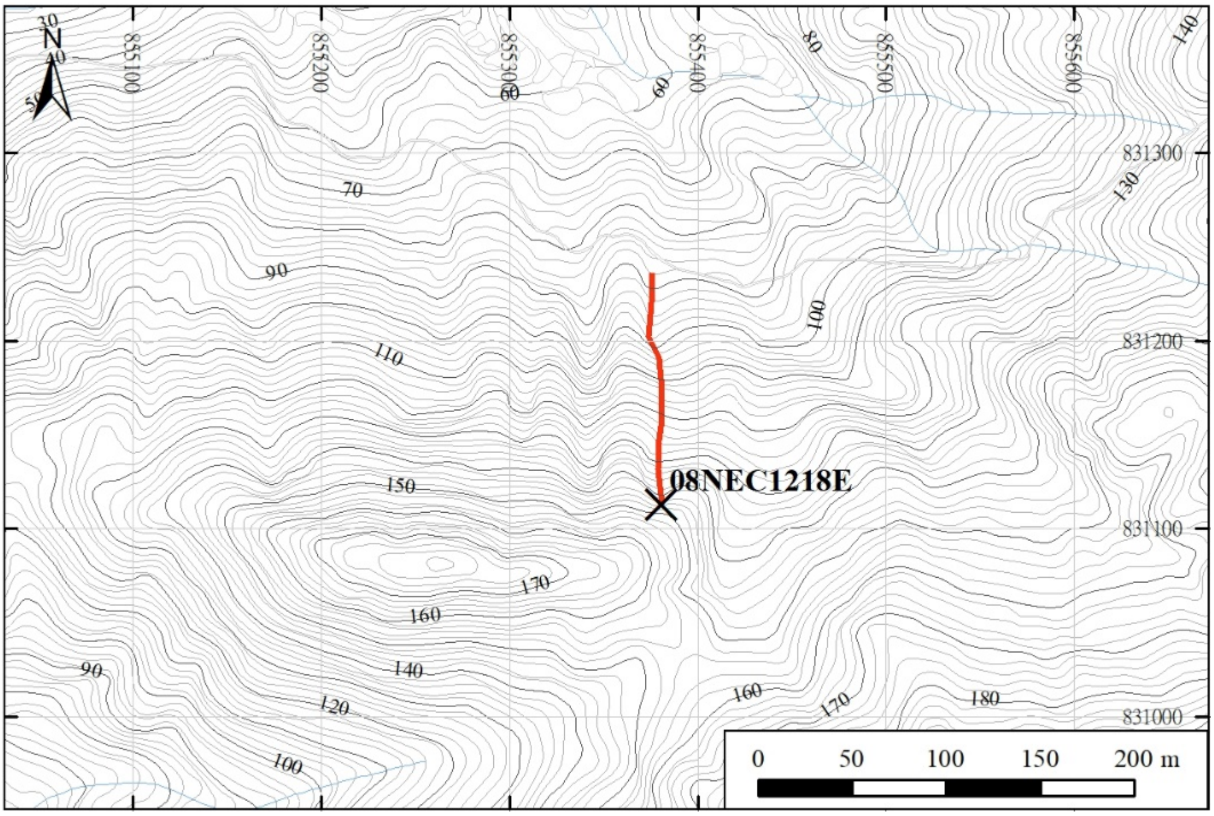

Location Plan of ENTLI No. 08NEC1218E

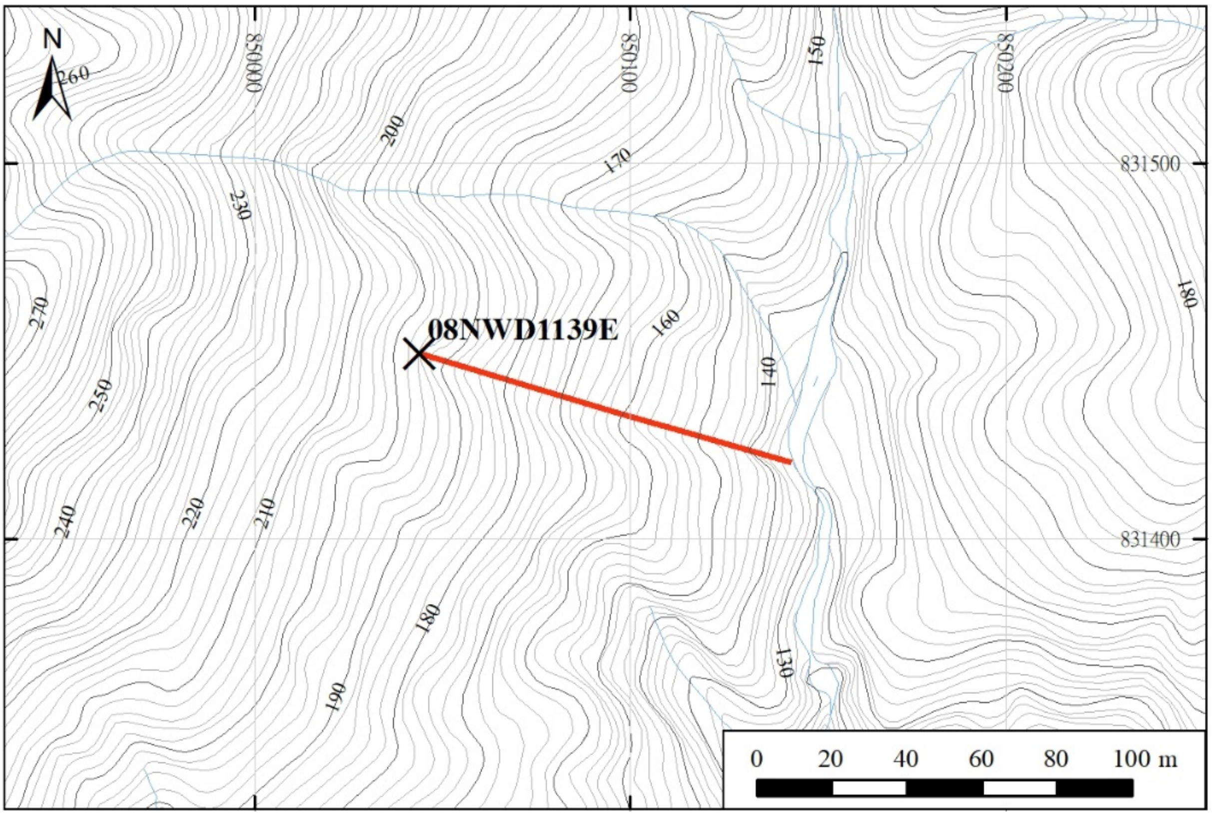

Location Plan of ENTLI No. 08NWD1139E

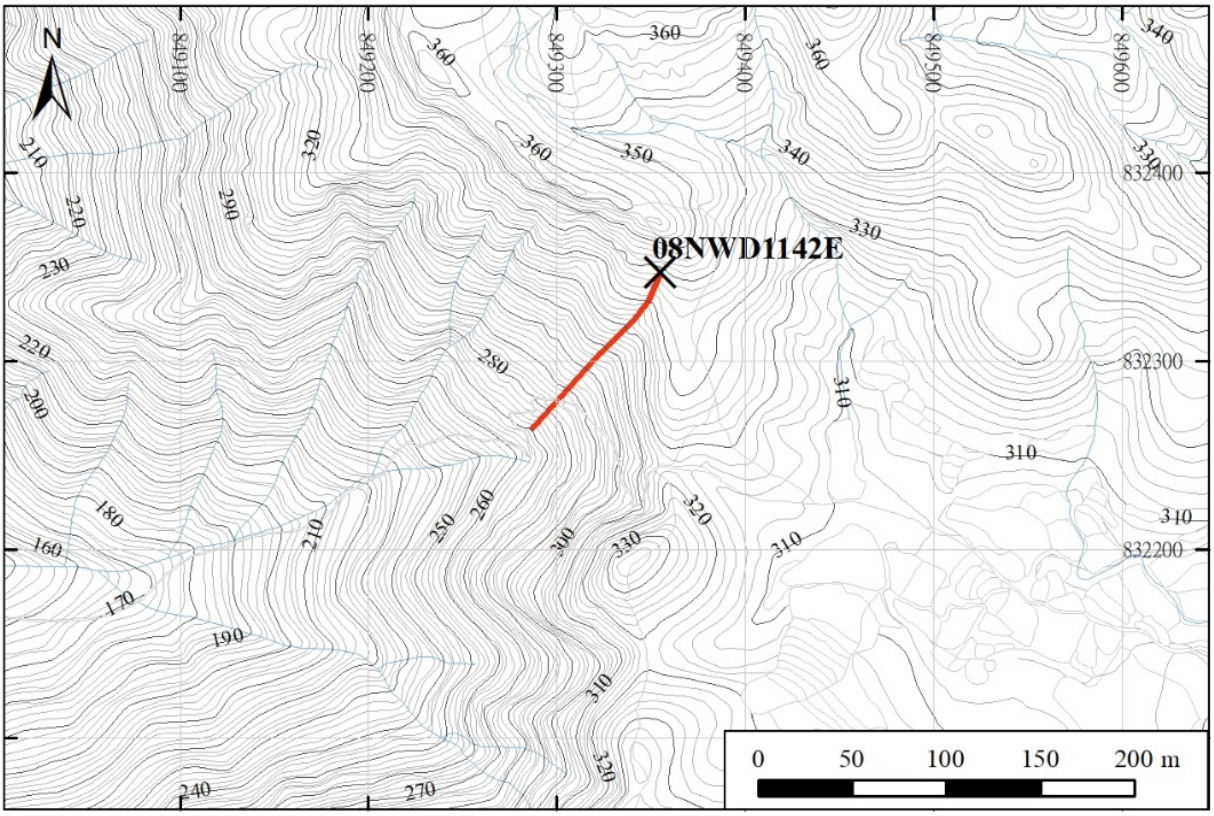

Location Plan of ENTLI No. 08NWD1142E

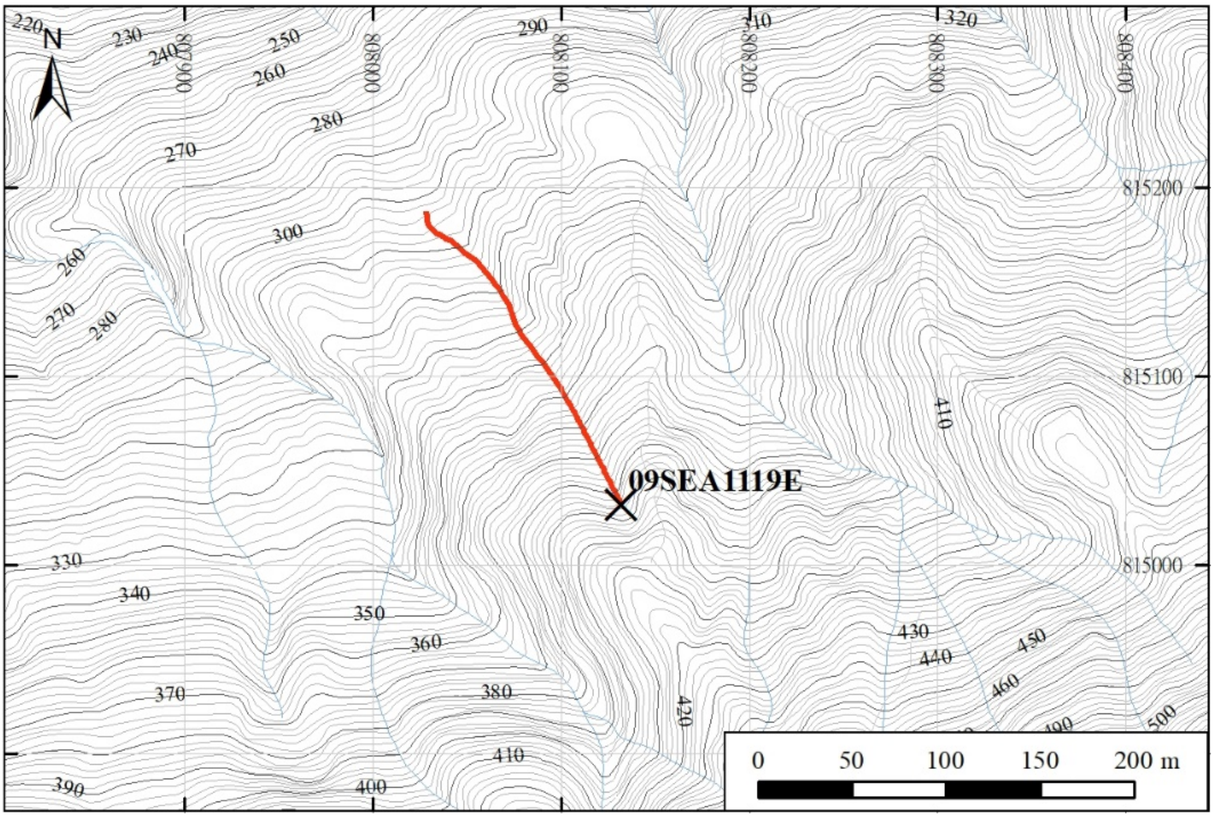

Location Plan of ENTLI No. 09SEA1119E

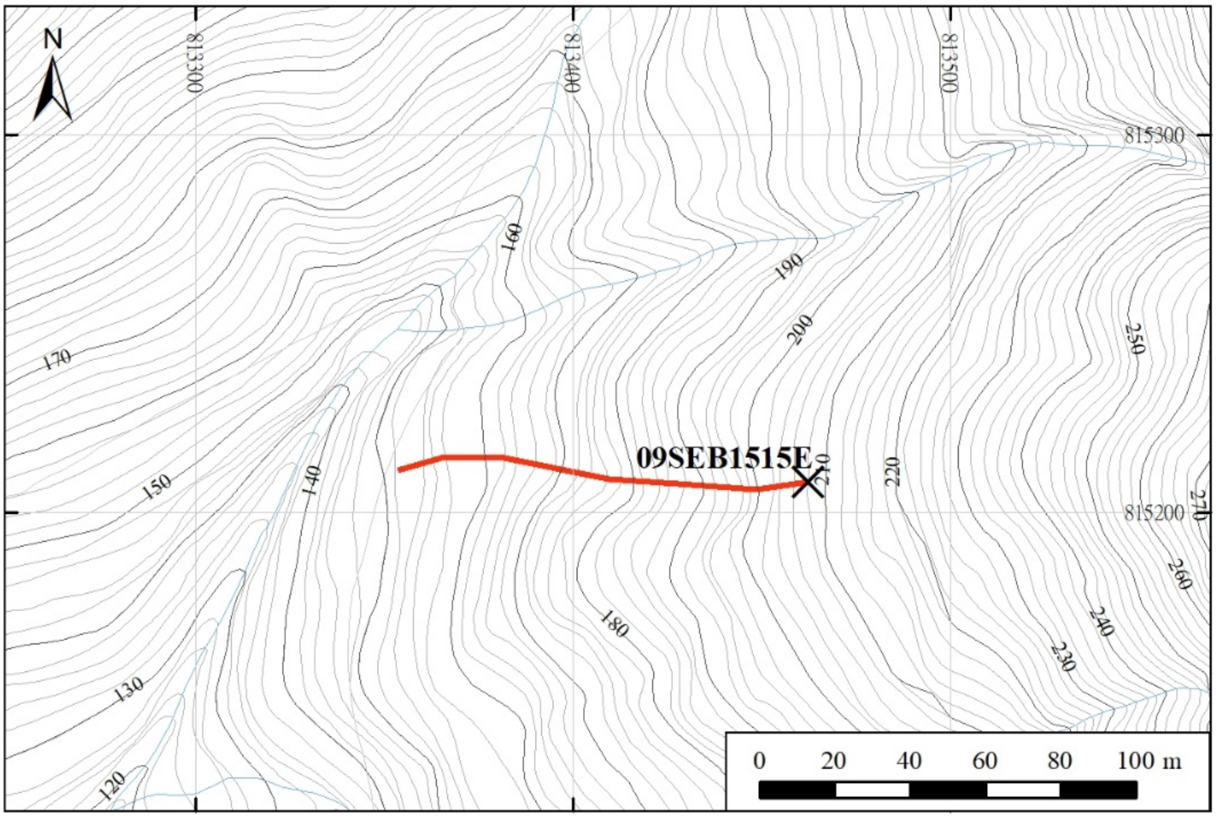

Location Plan of ENTLI No. 09SEB1515E

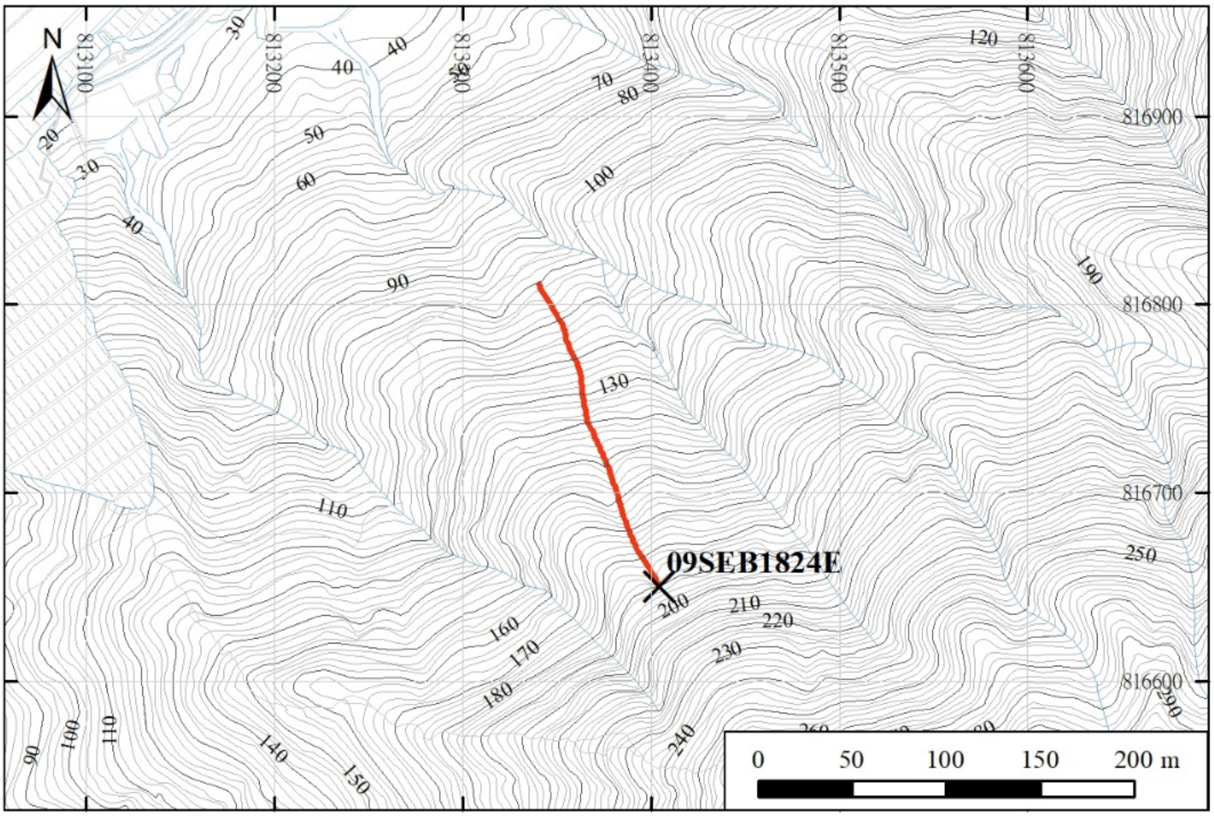

Location Plan of ENTLI No. 09SEB1824E

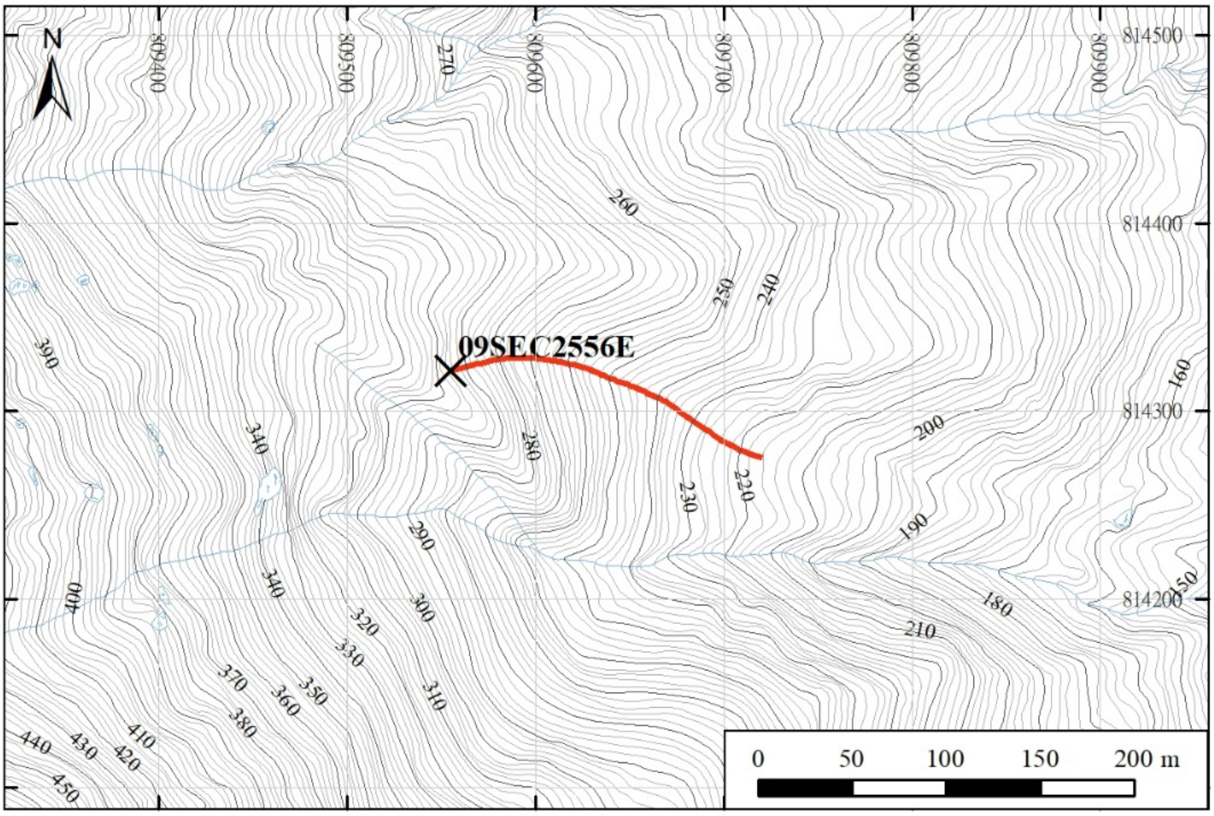

Location Plan of ENTLI No. 09SEC2556E

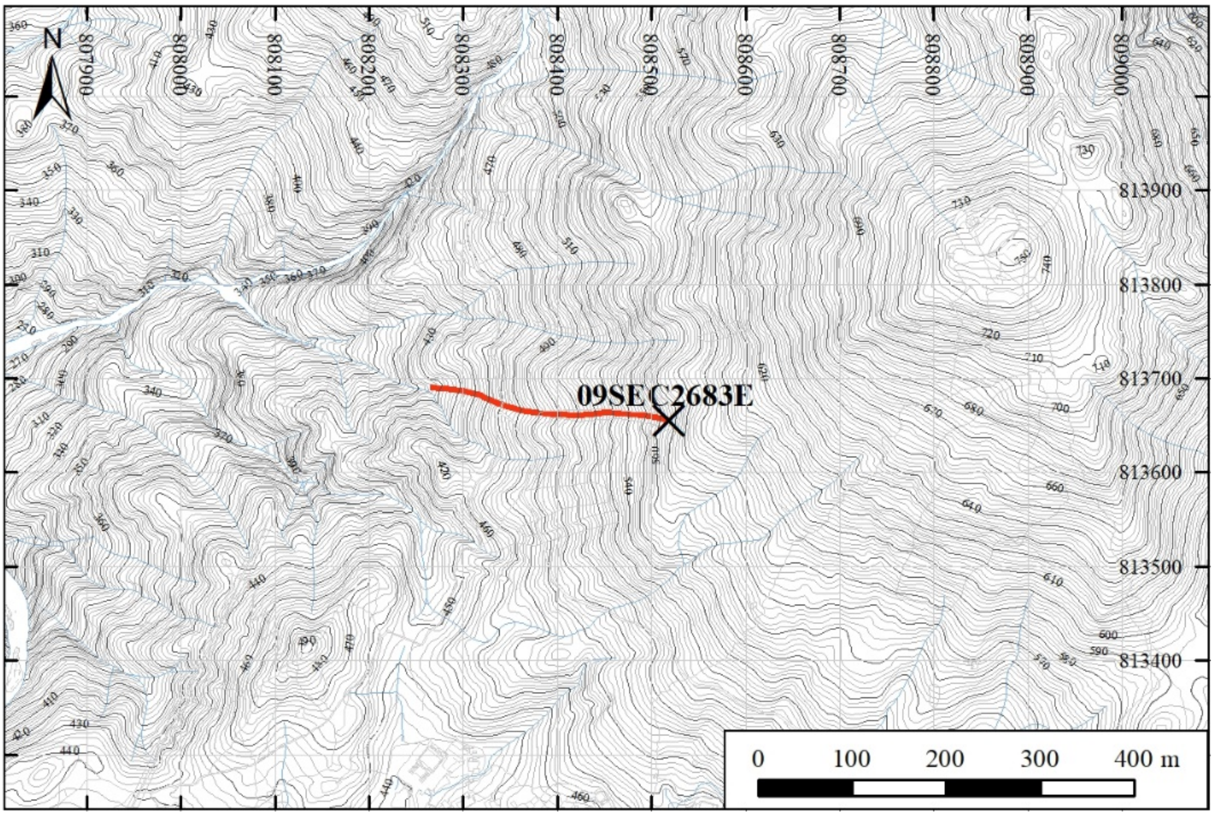

Location Plan of ENTLI No. 09SEC2683E

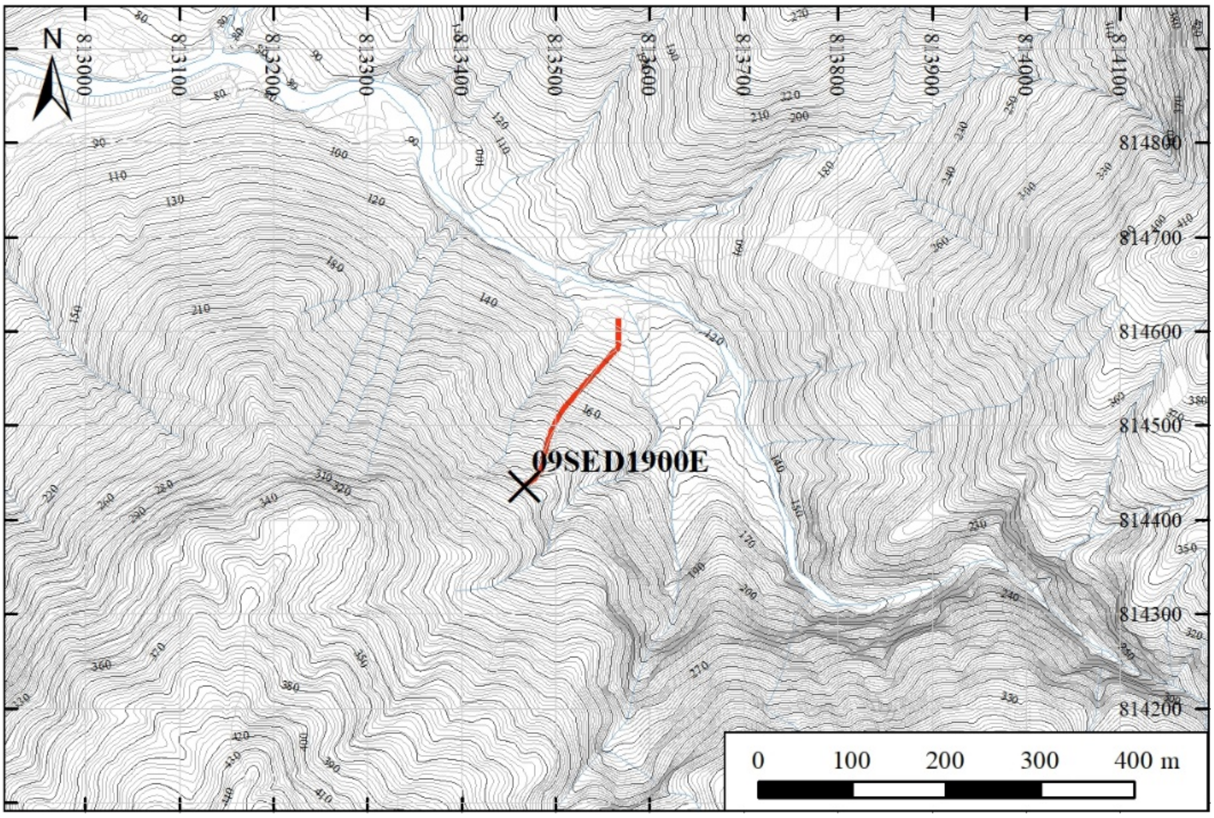

Location Plan of ENTLI No. 09SED1900E

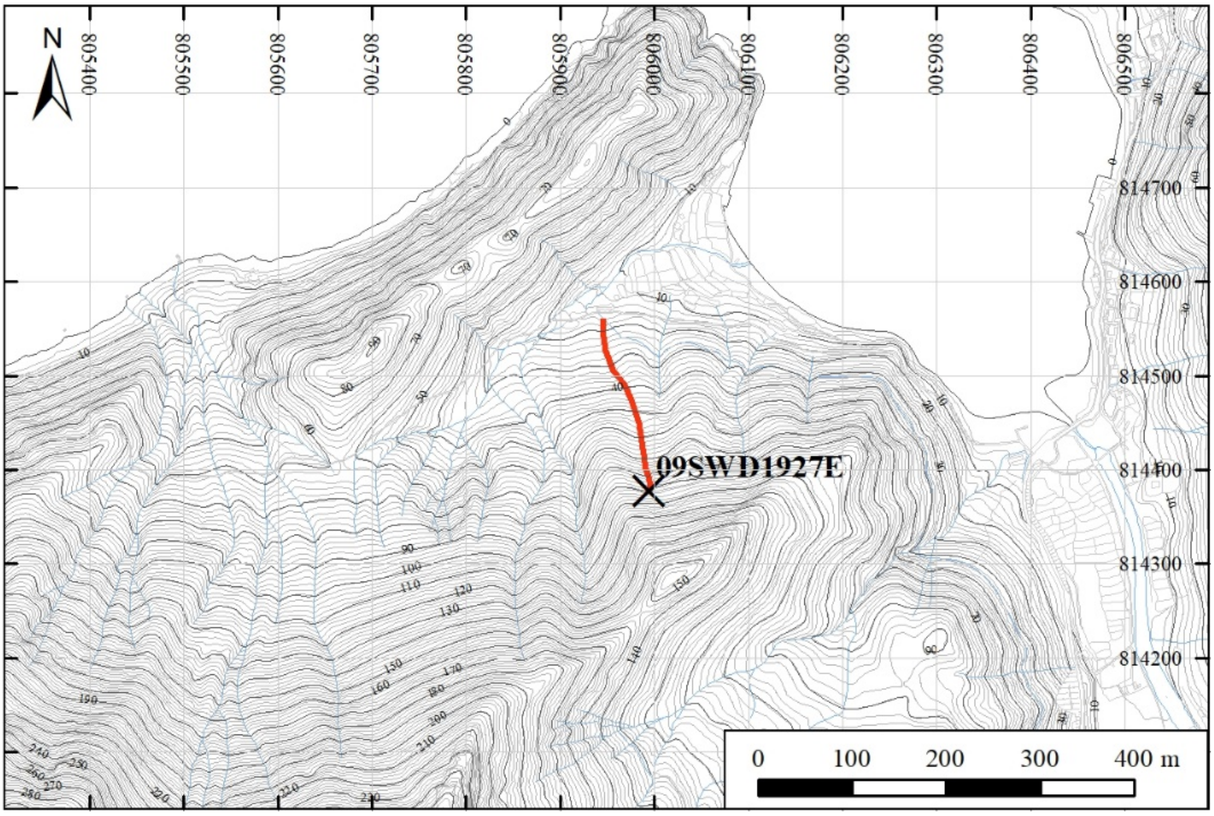

Location Plan of ENTLI No. 09SWD1927E

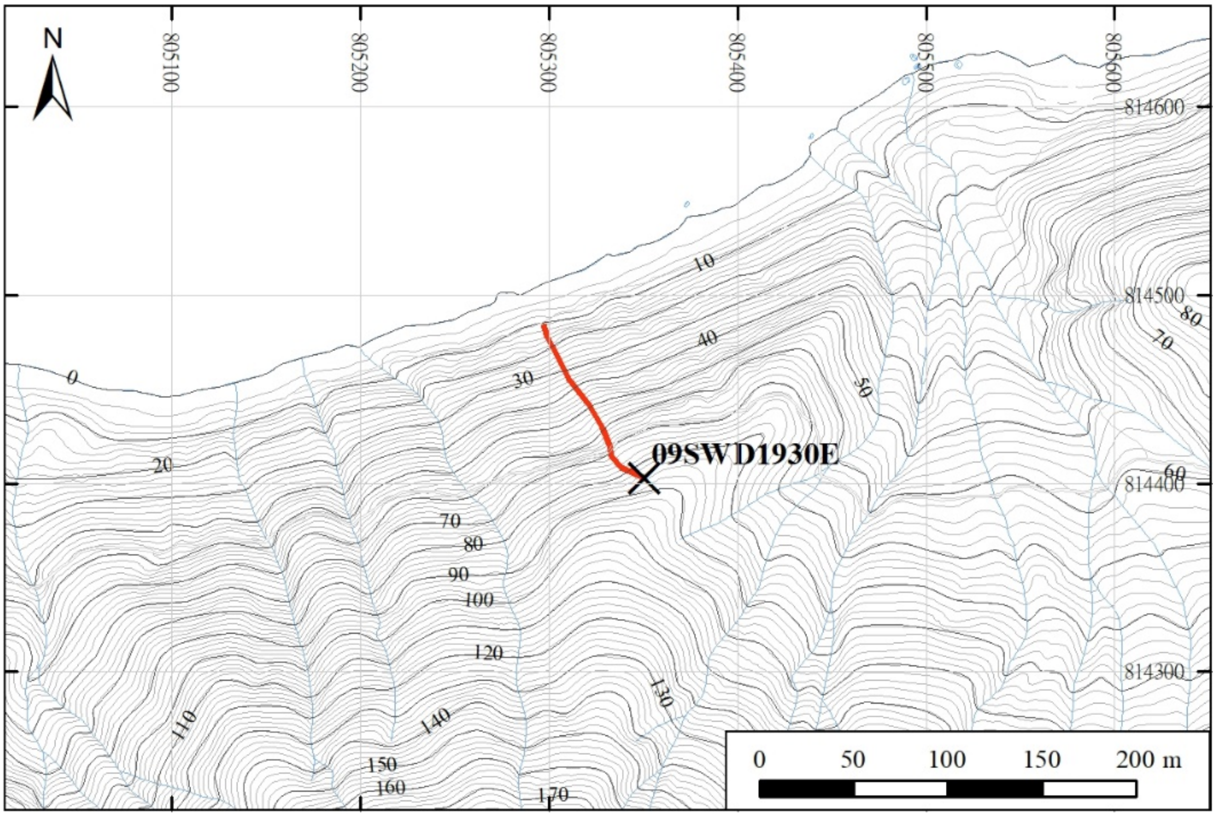

Location Plan of ENTLI No. 09SWD1930E

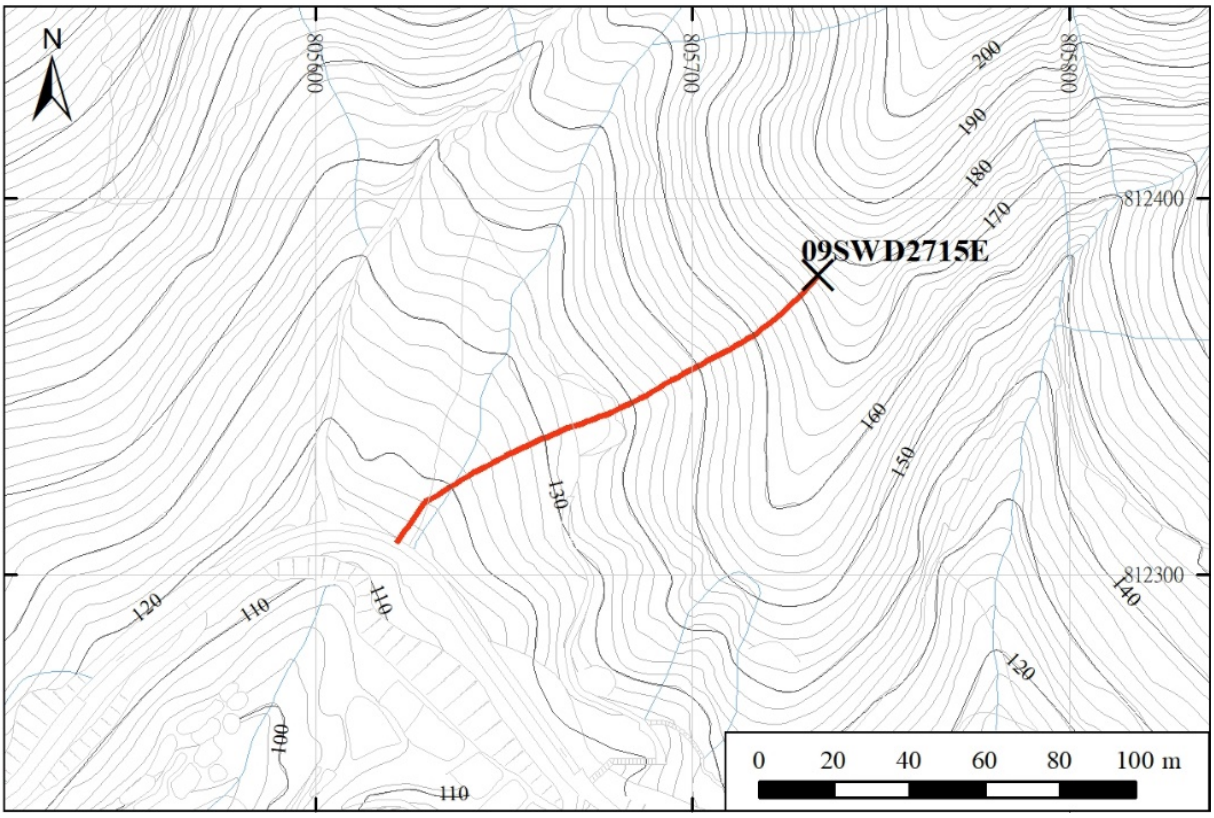

Location Plan of ENTLI No. 09SWD2715E

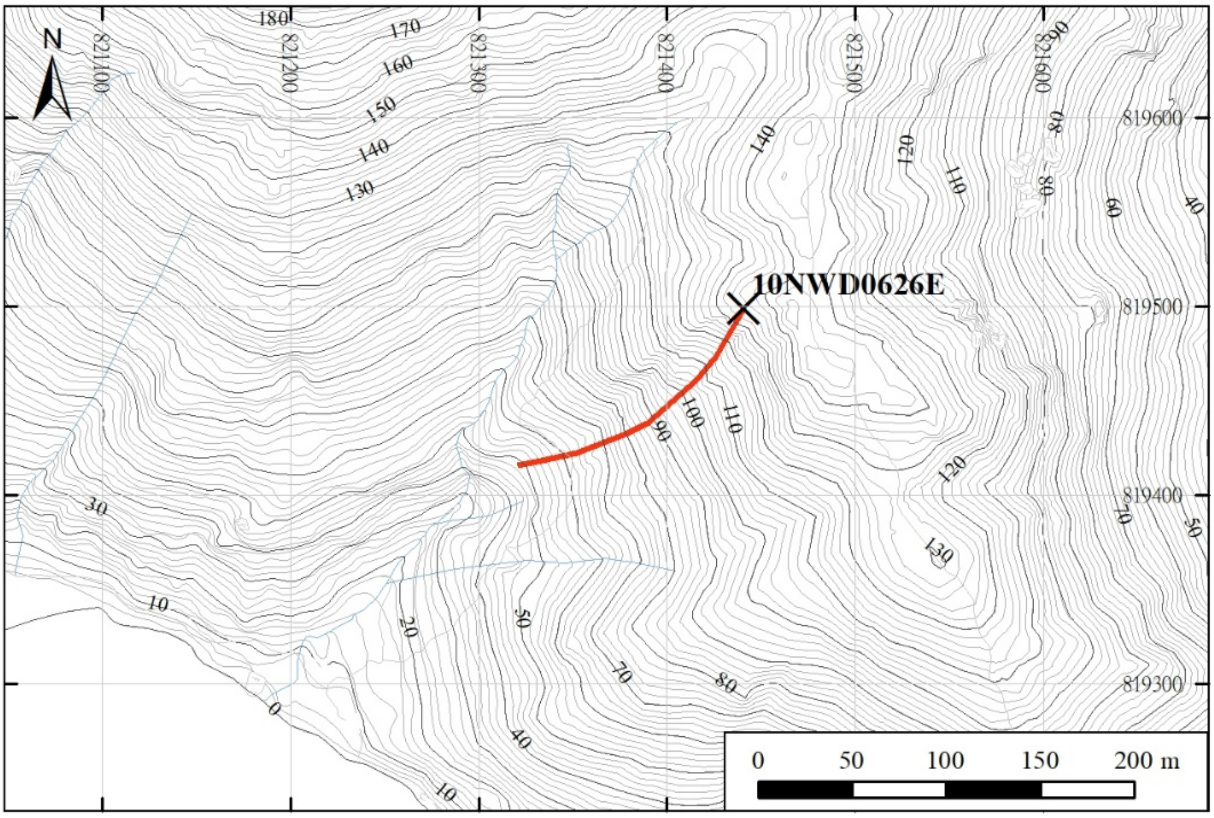

Location Plan of ENTLI No. 10NWD0626E

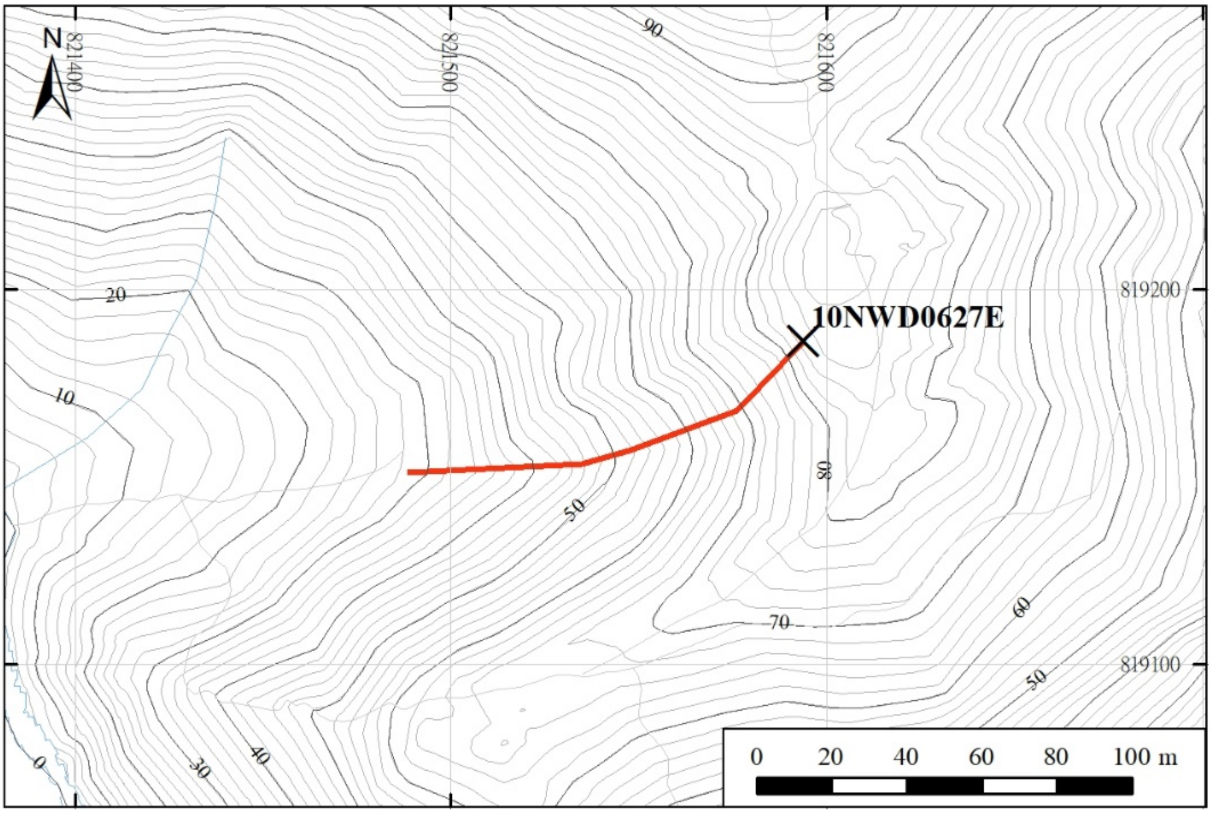

Location Plan of ENTLI No. 10NWD0627E

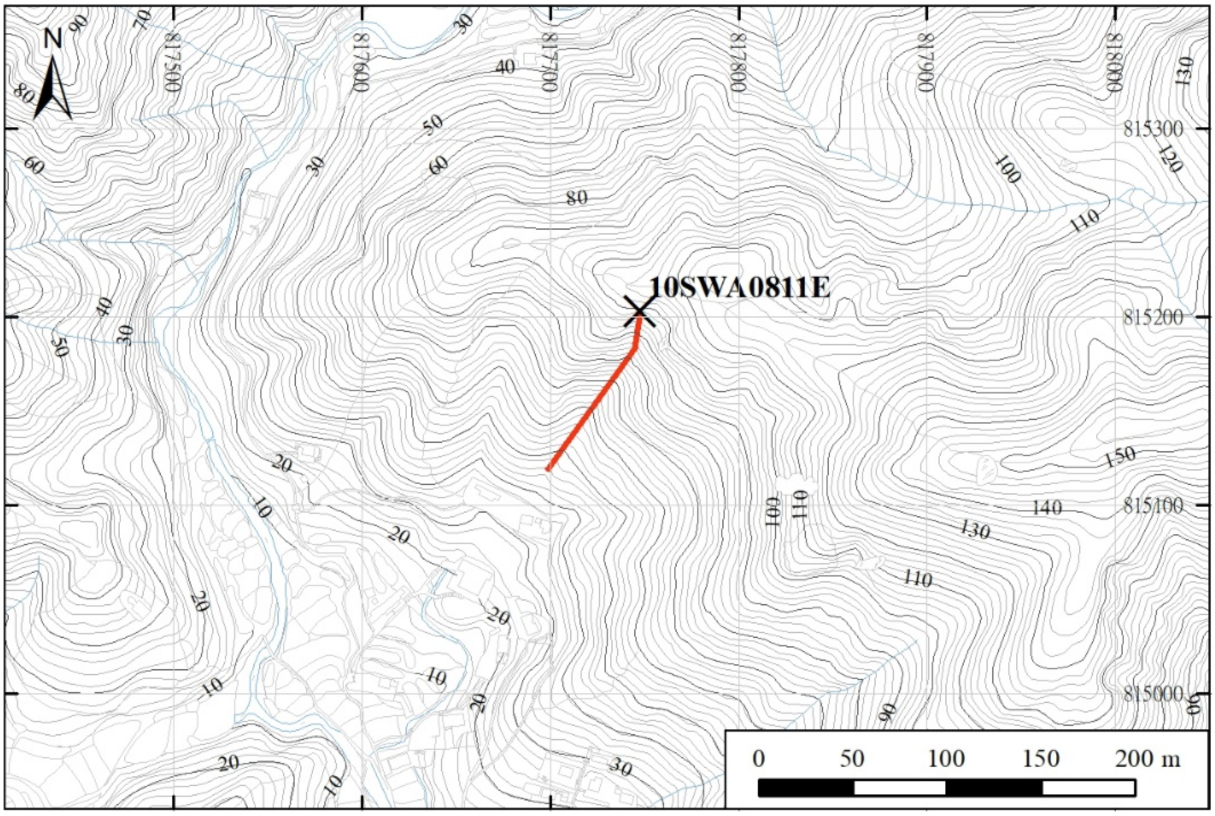

Location Plan of ENTLI No. 10SWA0811E

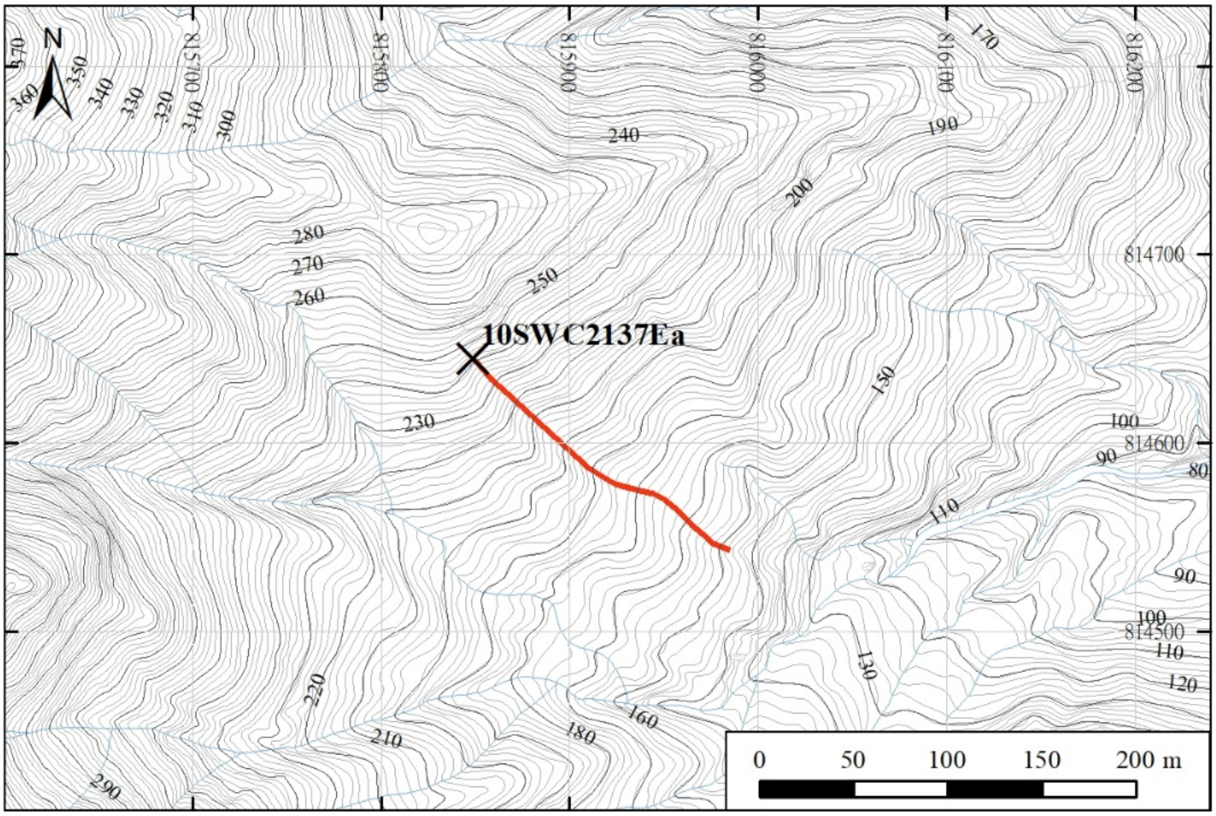

Location Plan of ENTLI No. 10SWC2137Ea

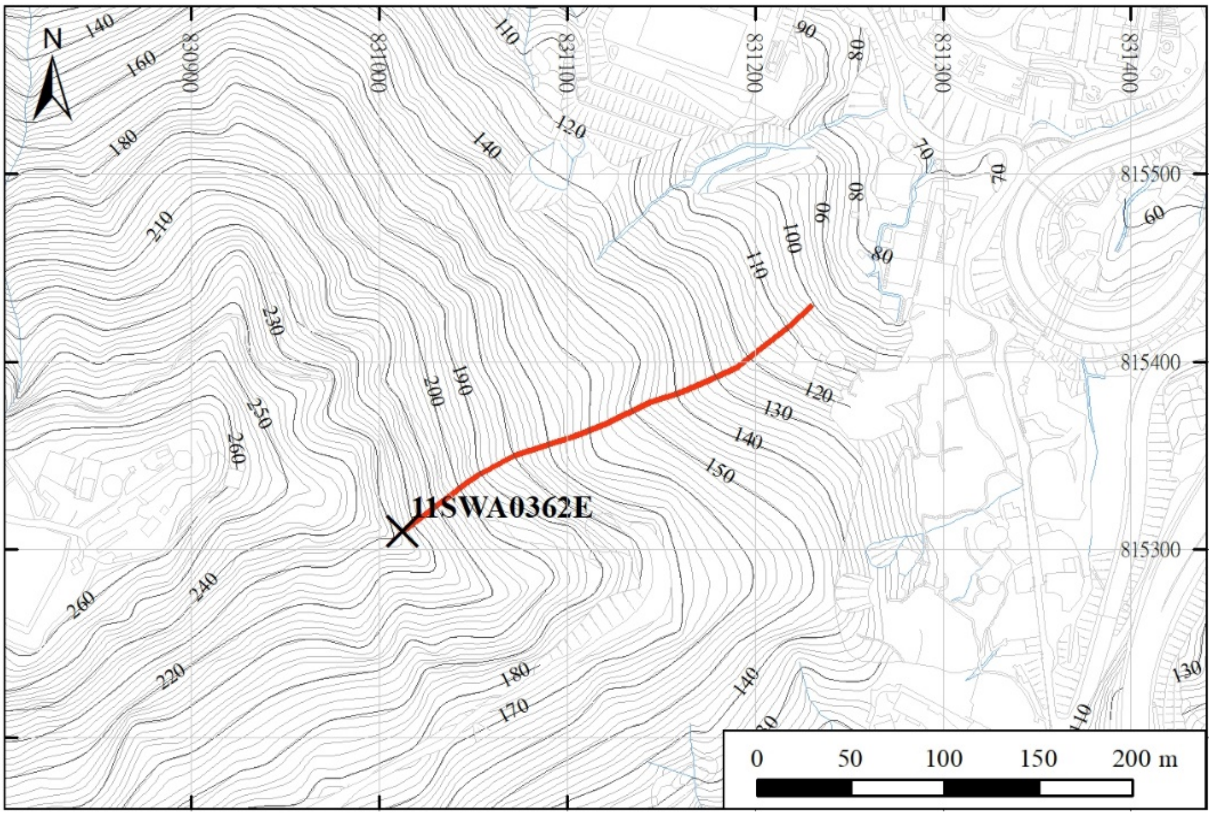

Location Plan of ENTLI No. 11SWA0362E

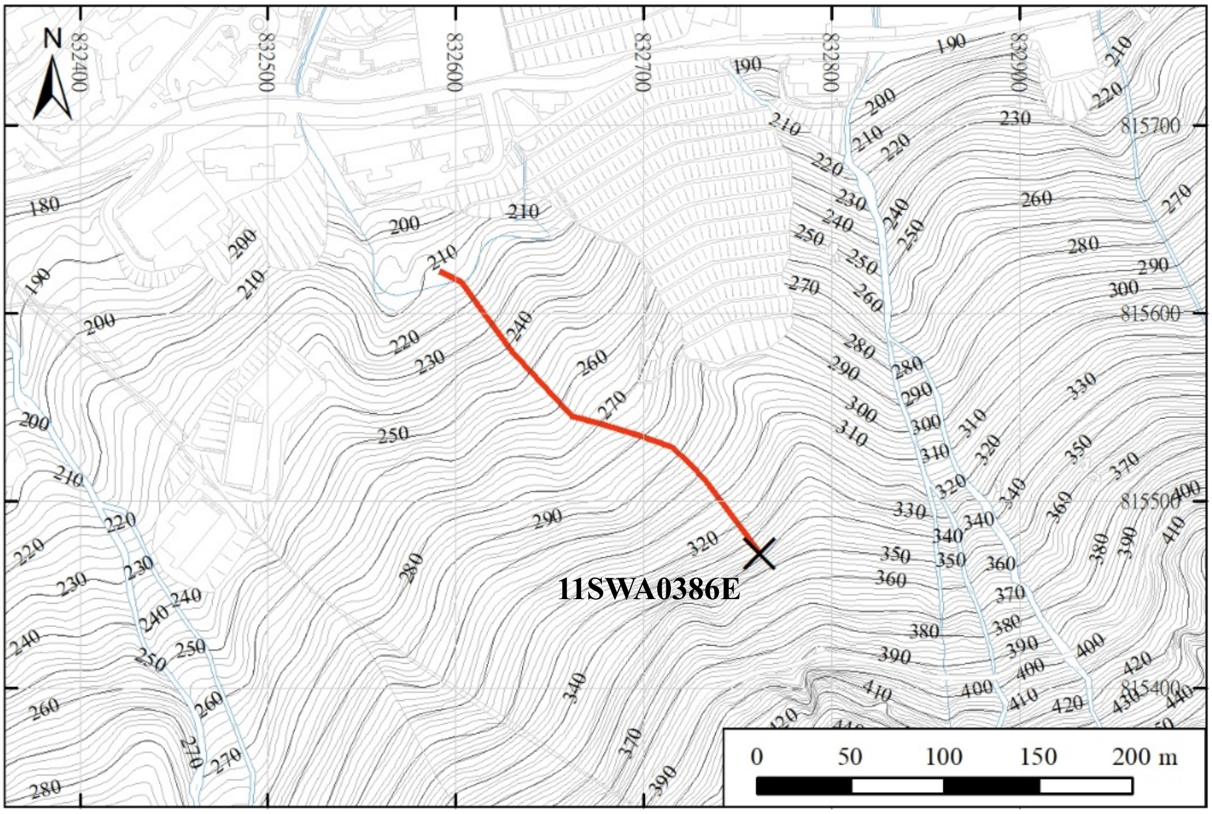

Location Plan of ENTLI No. 11SWA0386E

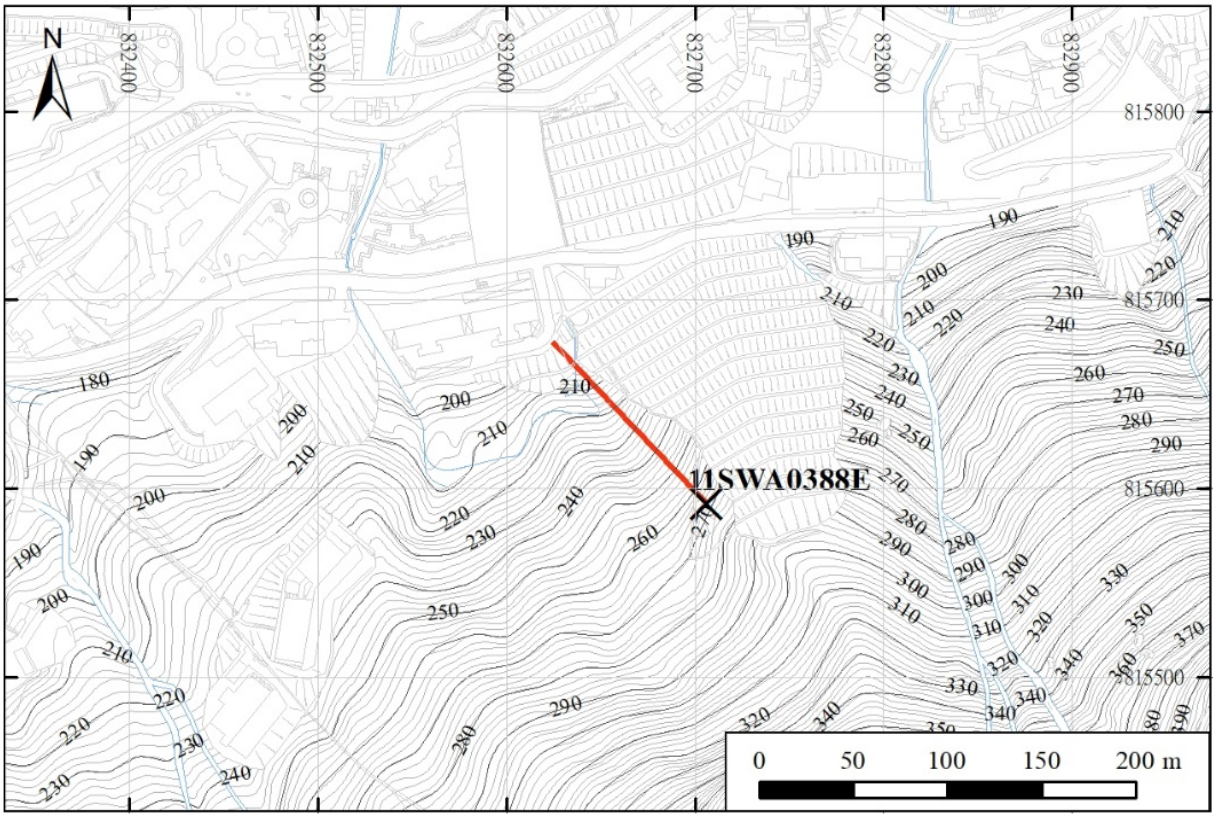

Location Plan of ENTLI No. 11SWA0388E

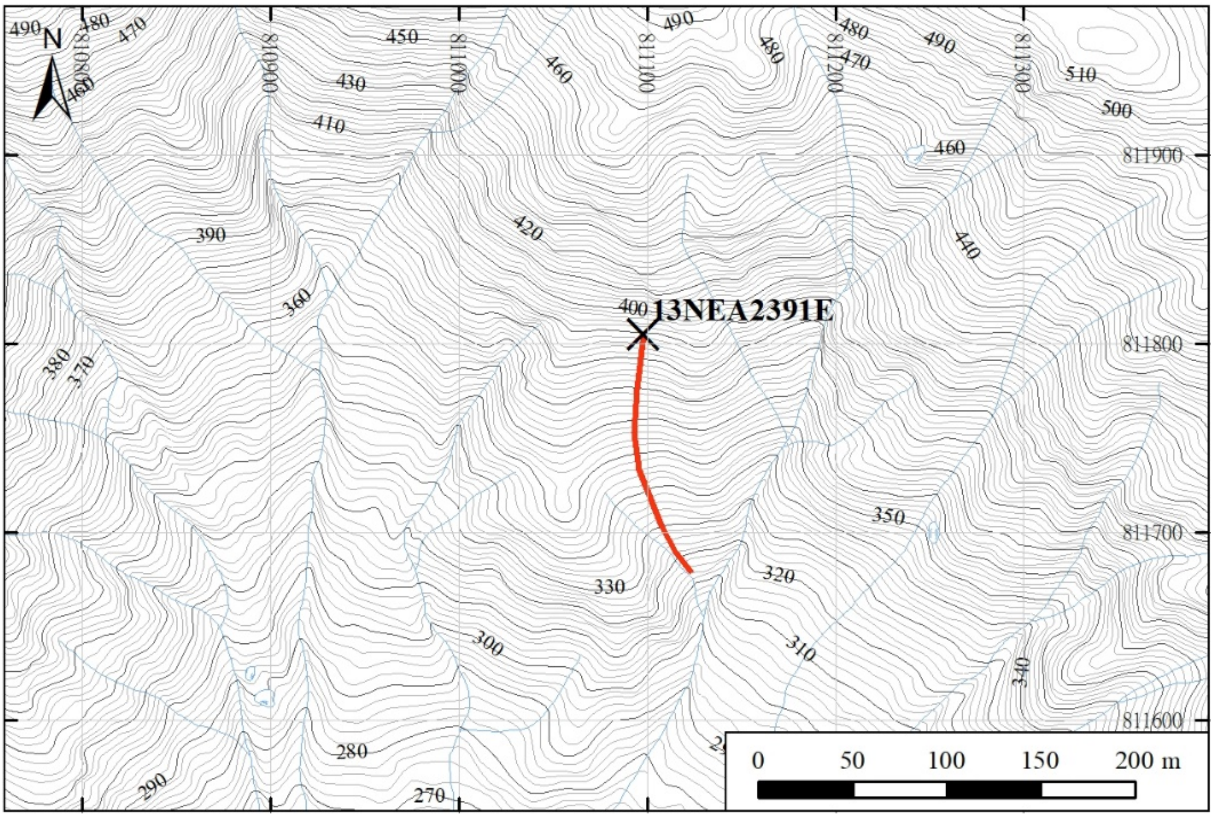

Location Plan of ENTLI No. 13NEA2391E

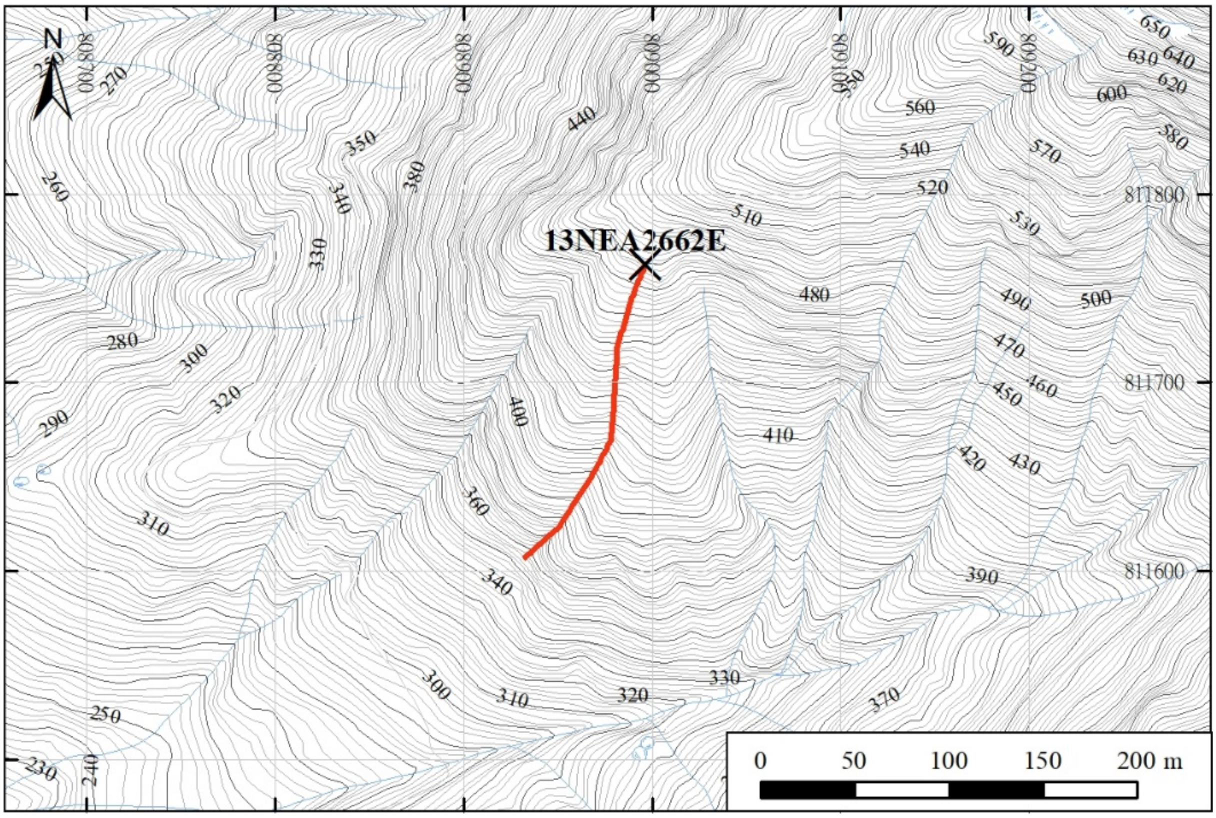

Location Plan of ENTLI No. 13NEA2662E

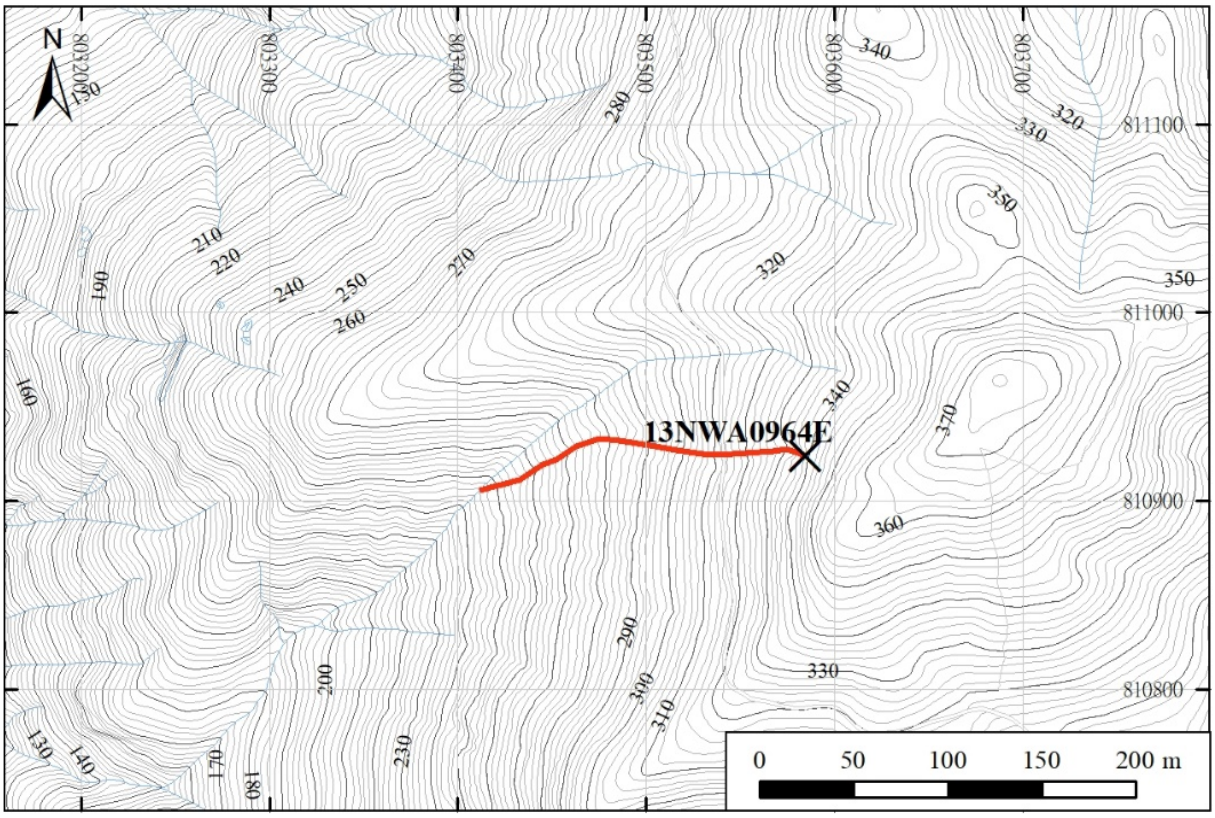

Location Plan of ENTLI No. 13NWA0964E

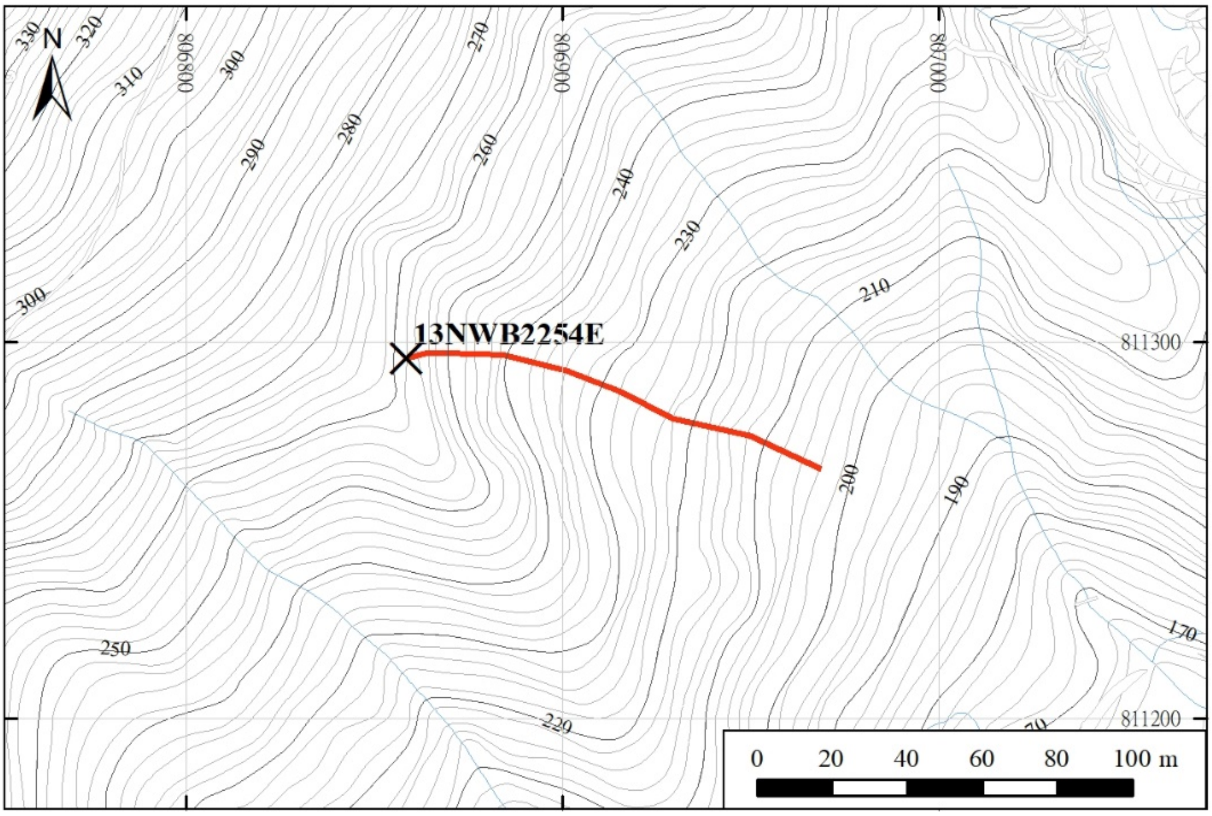

Location Plan of ENTLI No. 13NWB2254E

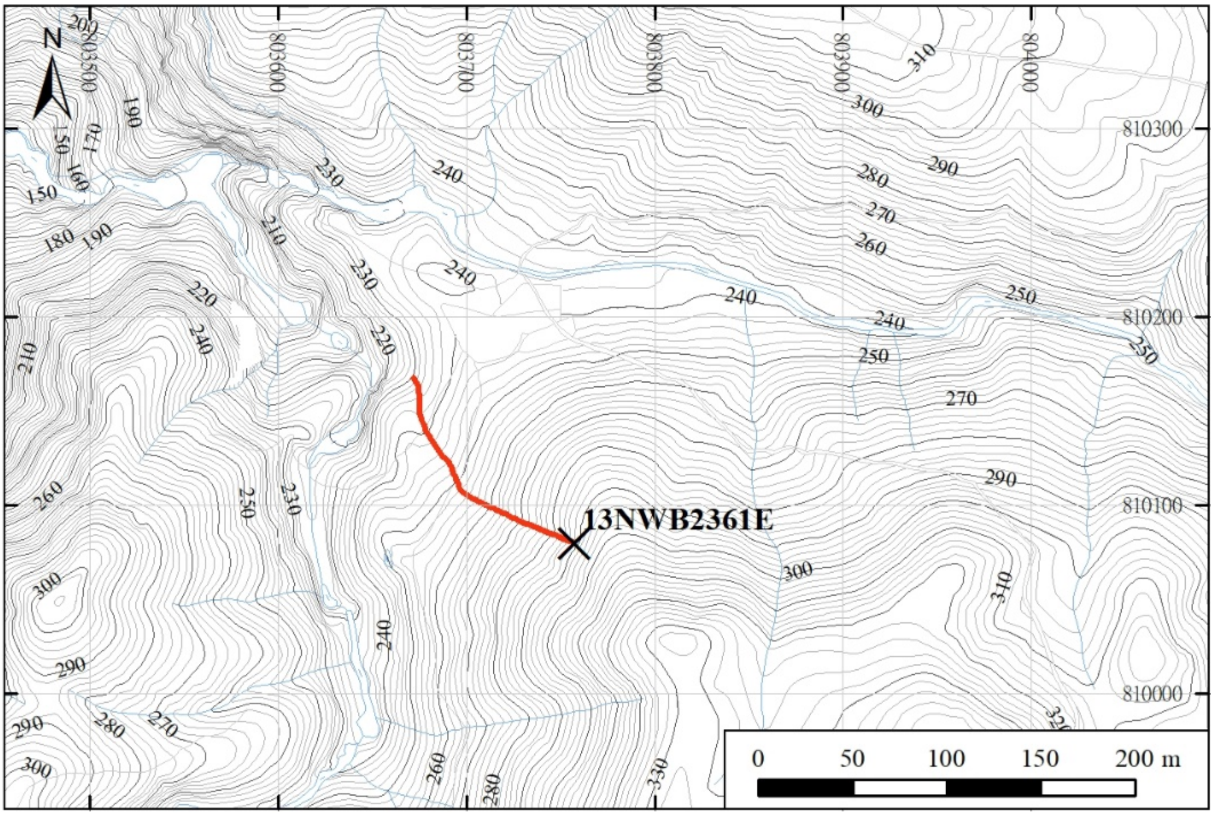

Location Plan of ENTLI No. 13NWB2361E

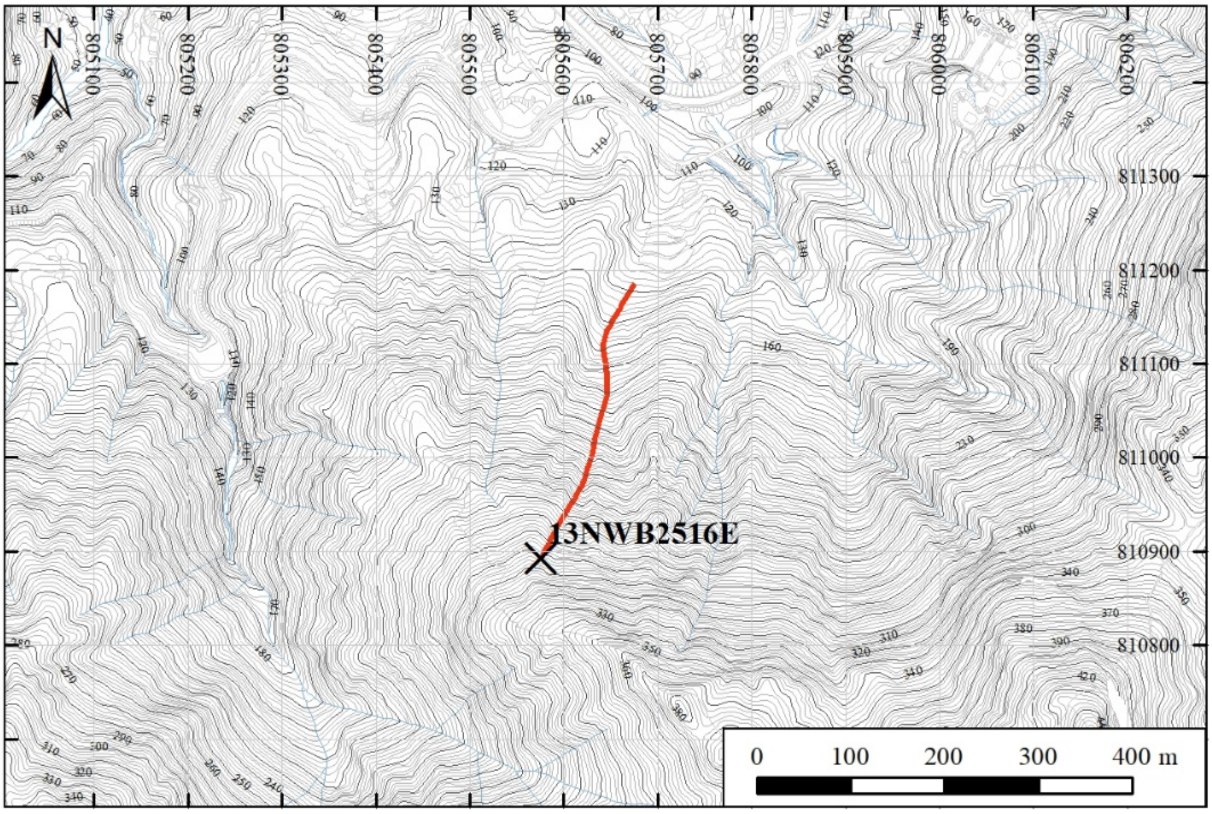

Location Plan of ENTLI No. 13NWB2516E

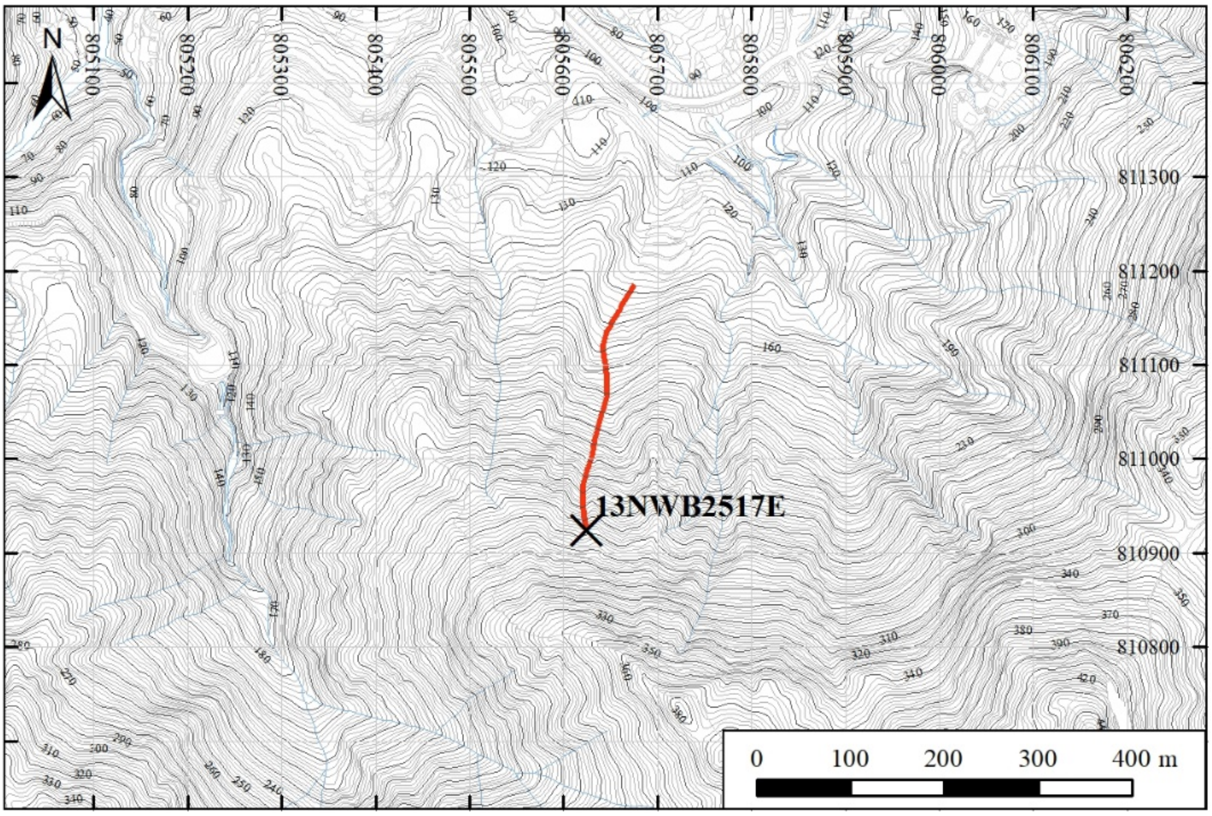

Location Plan of ENTLI No. 13NWB2517E

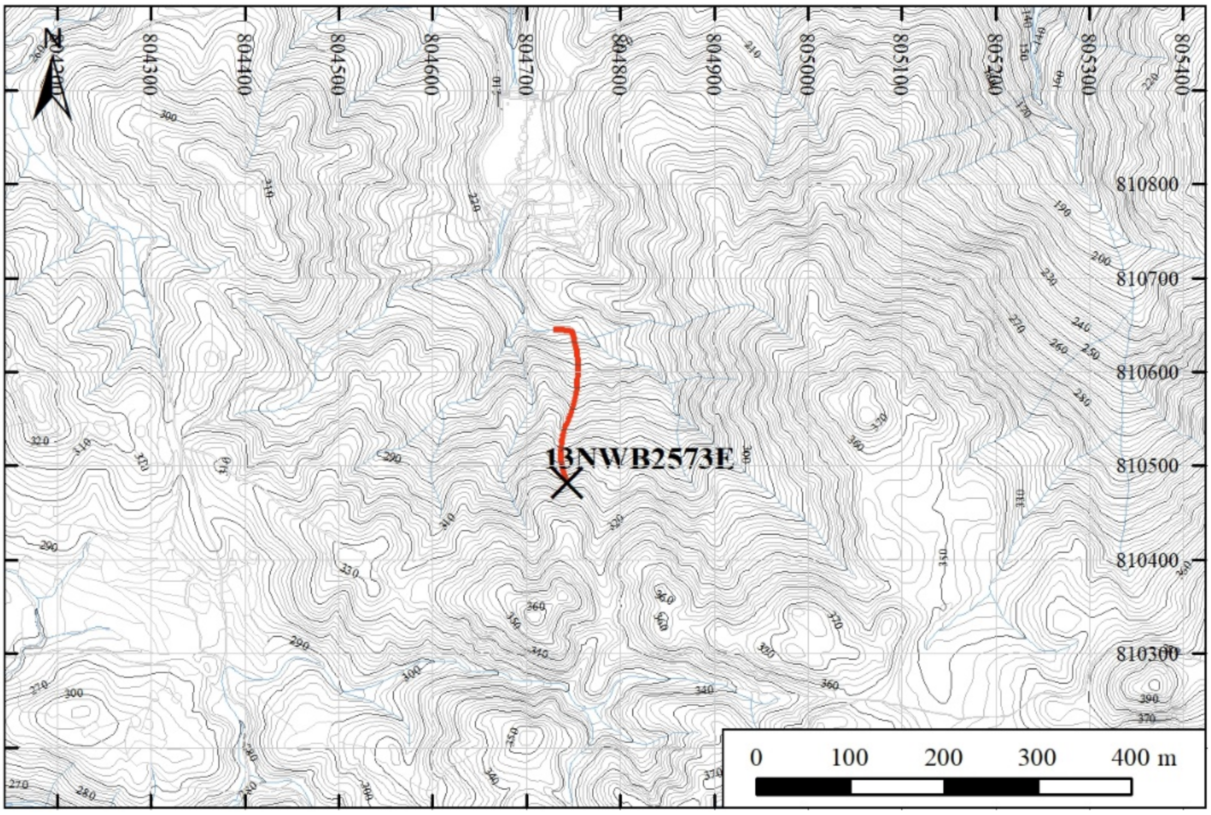

Location Plan of ENTLI No. 13NWB2573E

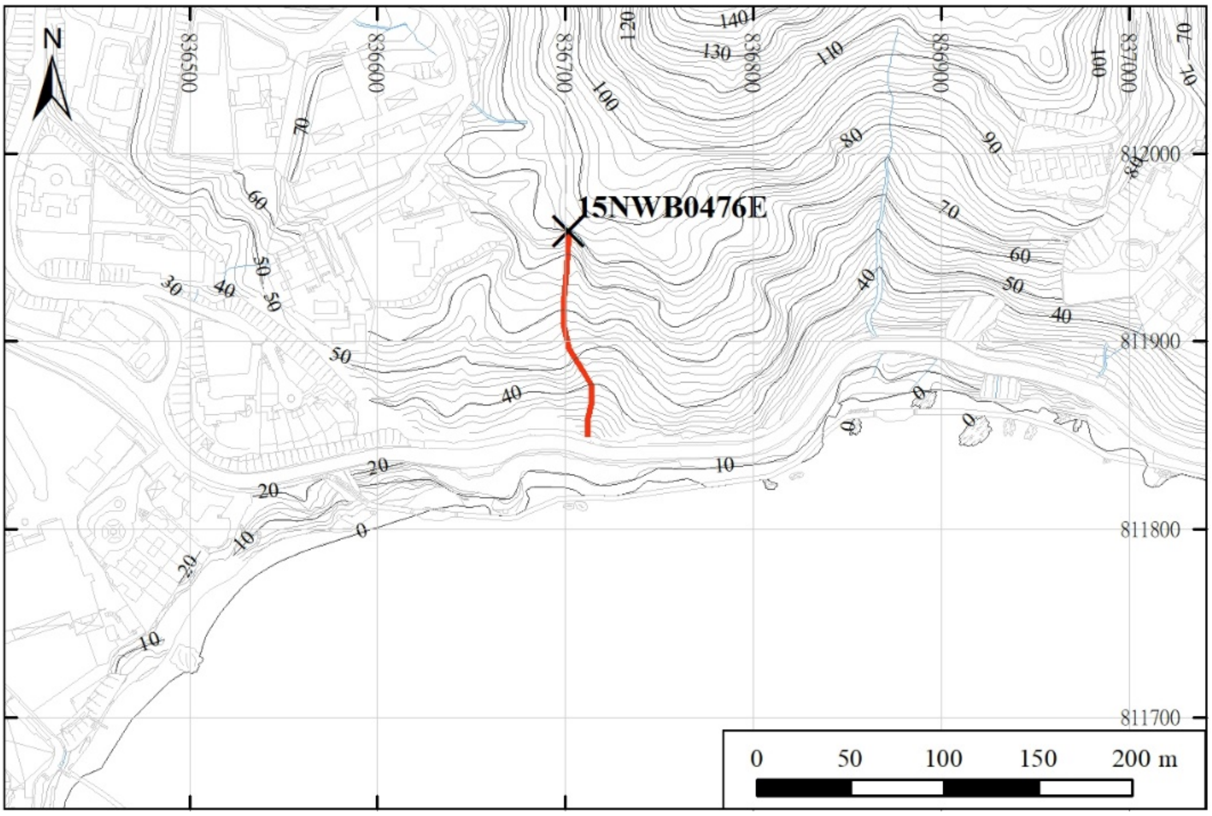

Location Plan of ENTLI No. 15NWB0476E

GEO PUBLICATIONS AND ORDERING INFORMATION
土力工程處刊物及訂購資料

An up-to-date full list of GEO publications can be found at the CEDD Website http://www.cedd.gov.hk on the Internet under "Publications". The following GEO publications can also be downloaded from the CEDD Website:

i. Manuals, Guides and Specifications
ii. GEO technical guidance notes
iii. GEO reports
iv. Geotechnical area studies programme
v. Geological survey memoirs
vi. Geological survey sheet reports

詳盡及最新的土力工程處刊物目錄，已登載於土木工程拓展署的互聯網網頁http://www.cedd.gov.hk 的"刊物"版面之內。以下的土力工程處刊物亦可於該網頁下載：

i. 指南、指引及規格
ii. 土力工程處技術指引
iii. 土力工程處報告
iv. 岩土工程地區研究計劃
v. 地質研究報告
vi. 地質調查圖表報告

Copies of some GEO publications (except geological maps and other publications which are free of charge) can be purchased either by:

Writing to
Publications Sales Unit,
Information Services Department,
Room 626, 6th Floor,
North Point Government Offices,
333 Java Road, North Point, Hong Kong.

or

- Calling the Publications Sales Section of Information Services Department (ISD) at (852) 2537 1910
- Visiting the online Government Bookstore at http:// www.bookstore.gov.hk
- Downloading the order form from the ISD website at http://www.isd.gov.hk and submitting the order online or by fax to (852) 2523 7195
- Placing order with ISD by e-mail at puborder@isd.gov.hk

讀者可採用以下方法購買部分土力工程處刊物(地質圖及免費刊物除外):

書面訂購
香港北角渣華道333號
北角政府合署6樓626室
政府新聞處
刊物銷售組

或

- 致電政府新聞處刊物銷售小組訂購 (電話：(852) 2537 1910)
- 進入網上「政府書店」選購，網址為 http://www.bookstore.gov.hk
- 透過政府新聞處的網站 (http://www.isd.gov.hk) 於網上遞交訂購表格，或將表格傳真至刊物銷售小組 (傳真：(852) 2523 7195)
- 以電郵方式訂購 (電郵地址：puborder@isd.gov.hk)

1:100 000, 1:20 000 and 1:5 000 geological maps can be purchased from:

Map Publications Centre/HK,
Survey & Mapping Office, Lands Department,
23th Floor, North Point Government Offices,
333 Java Road, North Point, Hong Kong.
Tel: (852) 2231 3187
Fax: (852) 2116 0774

讀者可於下列地點購買1:100 000、1:20 000及1:5 000地質圖：

香港北角渣華道333號
北角政府合署23樓
地政總署測繪處
電話: (852) 2231 3187
傳真: (852) 2116 0774

Any enquires on GEO publications should be directed to:

Chief Geotechnical Engineer/Standards and Testing,
Geotechnical Engineering Office,
Civil Engineering and Development Department,
Civil Engineering and Development Building,
101 Princess Margaret Road,
Homantin, Kowloon, Hong Kong.
Tel: (852) 2762 5351
Fax: (852) 2714 0275
E-mail: ivanli@cedd.gov.hk

如對本處刊物有任何查詢，請致函：

香港九龍何文田公主道101號
土木工程拓展署大樓
土木工程拓展署
土力工程處
標準及測試部總土力工程師
電話: (852) 2762 5351
傳真: (852) 2714 0275
電子郵件: ivanli@cedd.gov.hk